RESEARCH ARTICLE

WILEY

Putative protective neural mechanisms in prereaders with a family history of dyslexia who subsequently develop typical reading skills

Xi Yu[1,2] | Jennifer Zuk[2] | Meaghan V. Perdue[2,3,4] | Ola Ozernov-Palchik[2,5] | Talia Raney[2] | Sara D. Beach[5,6] | Elizabeth S. Norton[7] | Yangming Ou[8,9,10] | John D. E. Gabrieli[5] | Nadine Gaab[2,11,12]

[1]State Key Laboratory of Cognitive Neuroscience and Learning, Beijing Normal University, Beijing, China

[2]Laboratories of Cognitive Neuroscience, Division of Developmental Medicine, Department of Medicine, Boston Children's Hospital, Boston, Massachusetts

[3]Department of Psychological Sciences, University of Connecticut, Storrs, Connecticut

[4]Haskins Laboratories, New Haven, Connecticut

[5]McGovern Institute for Brain Research, Massachusetts Institute of Technology, Cambridge, Massachusetts

[6]Division of Medical Sciences, Harvard University, Cambridge, Massachusetts

[7]Department of Communication Sciences and Disorders, Northwestern University, Evanston, Illinois

[8]Division of Newborn Medicine, Boston Children's Hospital, Boston, Massachusetts

[9]Fetal-Neonatal Neuroimaging and Developmental Science Center, Boston Children's Hospital, Boston, Massachusetts

[10]Department of Radiology, Boston Children's Hospital, Boston, Massachusetts

[11]Department of Pediatrics, Harvard Medical School, Boston, Massachusetts

[12]Harvard Graduate School of Education, Cambridge, Massachusetts

Correspondence
Xi Yu, PhD, State Key Laboratory of Cognitive Neuroscience and Learning, Beijing Normal University, Beijing 100875, China.
Email: xi.yu@bnu.edu.cn

Abstract

Developmental dyslexia affects 40–60% of children with a familial risk (FHD+) compared to a general prevalence of 5–10%. Despite the increased risk, about half of FHD+ children develop typical reading abilities (FHD+Typical). Yet the underlying neural characteristics of favorable reading outcomes in at-risk children remain unknown. Utilizing a retrospective, longitudinal approach, this study examined whether putative protective neural mechanisms can be observed in FHD+Typical at the prereading stage. Functional and structural brain characteristics were examined in 47 FHD+ prereaders who subsequently developed typical (n = 35) or impaired (n = 12) reading abilities and 34 controls (FHD−Typical). Searchlight-based multivariate pattern analyses identified distinct activation patterns during phonological processing between FHD+Typical and FHD−Typical in right inferior frontal gyrus (RIFG) and left temporo-parietal cortex (LTPC) regions. Follow-up analyses on group-specific classification patterns demonstrated LTPC hypoactivation in FHD+Typical compared to FHD−Typical, suggesting this neural characteristic as an FHD+ phenotype. In contrast, RIFG showed hyperactivation in FHD+Typical than FHD−Typical,

and its activation pattern was positively correlated with subsequent reading abilities in FHD+ but not controls (FHD−Typical). RIFG hyperactivation in FHD+Typical was further associated with increased interhemispheric functional and structural connectivity. These results suggest that some protective neural mechanisms are already established in FHD+Typical prereaders supporting their typical reading development.

1 | INTRODUCTION

Developmental dyslexia (dyslexia) is a neurodevelopmental learning disability that is characterized by difficulties with speed and accuracy of word reading, deficient decoding abilities, and poor spelling (IDA, 2007). Dyslexia has further been associated with functional and structural alterations in primarily left-hemispheric reading network components comprising the frontal, temporo-parietal and occipito-temporal areas that underlie typical reading abilities (McCandliss & Noble, 2003; Norton, Beach, & Gabrieli, 2015; Ozernov-Palchik, Yu, Wang, & Gaab, 2016; Pugh et al., 2000; Richlan, Kronbichler, & Wimmer, 2009, 2011, 2013). Children with dyslexia often experience severe difficulties in their academic and personal lives as well as mental health due to the importance of reading in school curricula and in society (Baker & Ireland, 2007; Dougherty, 2003; Morgan, Fuchs, Compton, Cordray, & Fuchs, 2008).

There is an increased familial occurrence of dyslexia, ranging from 40 to 60%, compared to a prevalence of around 5–10% in the general population (Astrom, Wadsworth, & DeFries, 2007; Katusic, Colligan, Barbaresi, Schaid, & Jacobsen, 2001; Snowling & Melby-Lervåg, 2016) and several susceptibility genes have been identified (e.g., Newbury et al., 2011; Poelmans, Buitelaar, Pauls, & Franke, 2011; Scerri et al., 2011; Taipale et al., 2003). Behavioral longitudinal studies have demonstrated early deficits in language and preliteracy skills (e.g., phonological processing and rapid automatized naming) in toddlers and preschoolers with (FHD+) compared to without (FHD−) a familial risk of dyslexia (e.g., Koster et al., 2005; Lyytinen et al., 2001, 2004; Plakas, van Zuijen, van Leeuwen, Thomson, & van der Leij, 2013; van der Leij et al., 2013). Moreover, FHD+ prereaders have shown atypical neural characteristics in brain regions important for reading development, such as alterations in gray matter of temporo-parietal and occipito-temporal regions (Hosseini et al., 2013; Im, Raschle, Smith, Ellen Grant, & Gaab, 2015; Raschle, Chang, & Gaab, 2011) and white matter metrics of fibers connecting these areas (Vandermosten et al., 2015; Wang et al., 2016), as well as disrupted neural responses during literacy activities (Maurer, Bucher, Brem, & Brandeis, 2003; Raschle, Stering, Meissner, & Gaab, 2013; Raschle, Zuk, & Gaab, 2012). These neural atypicalities have been observed as early as in infancy (e.g., Guttorm, Leppänen, Richardson, & Lyytinen, 2001; Langer et al., 2017; Leppänen, Pihko, Eklund, & Lyytinen, 1999; van Herten et al., 2008; van Leeuwen et al., 2006, also see Ozernov-Palchik & Gaab, 2016 for a review). The early emergence of

cognitive and neural alterations in FHD+ children suggests that the observed alterations might serve as developmental mechanisms that contribute to dyslexia susceptibility instead of resulting from reduced language and/or reading experiences (e.g., Lyytinen et al., 2001; Raschle, Zuk, & Gaab, 2012; Snowling & Melby-Lervåg, 2016). Nevertheless, approximately half of FHD+ children subsequently develop typical reading skills (Gallagher, Frith, & Snowling, 2000; Pennington & Lefly, 2001; Scarborough, 1990; Snowling, Gallagher, & Frith, 2003; Snowling & Melby-Lervåg, 2016; Torppa, Lyytinen, Erskine, Eklund, & Lyytinen, 2010). Previously, longitudinal behavioral studies have identified several protective factors in FHD+ prereaders that support their subsequent typical reading development. These positive factors include enhanced oral language abilities, particularly in vocabulary knowledge and syntactic structure, and increased executive functioning skills (e.g., Haft, Myers, & Hoeft, 2016; Plakas et al., 2013; Snowling et al., 2003; Snowling & Melby-Lervåg, 2016; Torppa et al., 2010). However, it remains unknown whether there are also protective mechanisms in the prereading brain that may facilitate typical reading development in FHD+Typical children.

Compensatory neural mechanisms have previously been investigated in older struggling readers after several years of formal reading instruction. These studies, in general, suggest that difficulties in learning to read in these children might be mediated by neural compensatory pathways involving the right-hemispheric (RH) network (Barquero, Davis, & Cutting, 2014). More specifically, increased activation in RH regions have been shown in compensated readers compared to those with persistently poor reading skills (Shaywitz et al., 2003) and in individuals who demonstrated reading improvement after successful interventions (e.g., Eden et al., 2004; Temple et al., 2003). Moreover, RH neural characteristics of struggling readers, such as increased neural activation in the right frontal cortex during phonological processing and stronger connectivity strength of the right white matter tracts important for reading, have also been shown to predict subsequent reading improvement (Farris, Ring, Black, Lyon, & Odegard, 2016; Hoeft et al., 2011). In addition, the compensatory role of the RH has further been observed in children with dyslexia, for which higher neural sensitivities for speech sounds have been associated with better phonological and reading skills (Lohvansuu et al., 2014).

In addition to the development of compensatory mechanisms in poor readers or children with dyslexia, which likely develop in response to successful reading intervention, it has been hypothesized that some children might already exhibit protective neural mechanisms in the right hemisphere at the prereading stage (Yu, Zuk, &

Gaab, 2018). This may enable them to develop typical reading skills that might be otherwise compromised due to atypical/alternative brain development associated with a familial risk of dyslexia. As a group, infants and children with a familial risk of dyslexia seem to show a greater predisposition for a bilateral/right-lateralized brain network supporting language and reading development, compared to controls who show a primarily left-hemispheric dominance (e.g., Guttorm et al., 2001; Leppänen et al., 1999; Lyytinen et al., 2005; van Herten et al., 2008; van Leeuwen et al., 2006; van Leeuwen et al., 2007; Wang et al., 2016; for reviews, also see Lyytinen et al., 2005 and Ozernov-Palchik & Gaab, 2016). For example, enhanced neural sensitivity to speech sounds in the right hemisphere has been observed in FHD+ compared to FHD− infants within the first couple days of life (Guttorm et al., 2001). Consistent with the bilateral reading network in children at familial risk, variants of dyslexia susceptibility genes have also been associated with white matter microstructure of the corpus callosum (CC; Darki, Peyrard-Janvid, Matsson, Kere, & Klingberg, 2012; Scerri et al., 2012). The CC is the major fiber connecting both hemispheres and plays a critical role in interhemispheric communication and brain lateralization (Aboitiz & Montiel, 2003; Hinkley et al., 2016). Therefore, it is possible that the atypical development of the CC might provide a structural foundation for greater connectivity between both hemispheres, which facilitates the recruitment of the right hemisphere for reading development (Yu, Zuk, & Gaab, 2018). Consistent with this hypothesis, in a recent longitudinal study examining white matter development from the prereading (before kindergarten entry) to the fluent reading stage (up to fifth grade), right lateralization in white matter tracts important for reading was observed in FHD+ compared to FHD− preschoolers (Wang et al., 2016). Importantly, a significantly higher rate of white matter development in the right hemisphere has been demonstrated in subsequent good versus poor readers within a group of FHD+ children, suggesting possible early neural compensatory mechanisms in the right hemisphere. However, it remains unclear whether these alternative RH neural pathways are only developed to compensate for the difficulties/impairments children encounter after they start to learn to read (i.e., *compensatory mechanisms*). Alternatively, they might already be in place prior to reading onset (e.g., at birth or in early childhood) in some FHD+ children and thereby provide a protective role from the start of learning to read (i.e., *protective mechanisms*; Yu, Zuk, & Gaab, 2018).

Alternatively, one could argue that typical reading development among FHD+Typical children may simply be the result of lower genetic liability compared to children who have a familial risk and exhibit reading impairment (FHD+Impaired; Snowling et al., 2003; Van Bergen et al., 2011). Behavioral studies tracking FHD+ and FHD− children longitudinally over the course of learning to read have indicated that the liability for dyslexia is a continuous variable among children with familial risk. Specifically, FHD+Impaired children have shown lower performance on the key precursors of dyslexia, including phonological awareness, automatized rapid naming skills, and letter knowledge, compared to FHD+Typical children. However, FHD+Typical children have also been shown to perform more poorly than FHD−Typical children on these preliteracy and reading measures

(Pennington & Lefly, 2001; Snowling & Melby-Lervåg, 2016), indicating that the liability for dyslexia is a continuum and not a dichotomous variable. Nevertheless, it is unknown whether (a) FHD+Typical children display the characteristic functional and structural brain alterations previously described for children with a diagnosis of dyslexia due to their genetic liability, (b) what the neural protective/compensatory mechanisms associated with typical reading development are, and (c) whether these potential mechanisms are present prior to reading onset, which would suggest a protective role.

Utilizing a retrospective, longitudinal approach, the current study is the first to investigate whether putative protective neural mechanisms emerge prior to reading onset in preschoolers and early kindergarteners with a familial risk of dyslexia who subsequently develop typical reading skills. Forty-seven children with a familial risk for dyslexia who subsequently developed either typical (FHD+Typical, n = 35) or impaired (FHD+Impaired, n = 12) reading skills as well as 34 control children (i.e., FHD−Typical) were selected from our longitudinal database. Participants were selected based on their reading performance, which was assessed after at least 2 years of reading instruction. Retrospective analyses of the behavioral, structural (diffusion), and functional (phonological processing) data collected at the prereading stage (before or at the beginning of kindergarten) were conducted. Whole-brain analyses were first conducted with the fMRI data of FHD+Typical and FHD−Typical children to explore potential group differences associated with familial risk status despite equivalent typical reading performance. Both a mass-univariate analysis and a searchlight multivariate pattern analysis (MVPA) was applied to capture any group effect in individual voxels and activation patterns across neighboring voxels, respectively. In regions showing distinct activation patterns between the FHD−Typical and FHD+Typical children, as identified by the MVPA, follow-up analyses were conducted to characterize the specific pattern associated with each group. Moreover, to clarify the specific roles of regions that were differentially recruited by FHD+Typical compared to the FHD−Typical children, associations between the identified patterns in each region and subsequent reading abilities were further examined in FHD+ and control participants. Regions that showed putative protective effects as revealed by the MVPA were applied as seeds in the subsequent functional connectivity (FC) analyses to investigate the network characteristics of these regions during phonological processing. Additionally, in order to explore white matter mechanisms underlying the putative RH protective pathways, FA values of RH tracts previously associated with reading skills (Horowitz-Kraus, Wang, Plante, & Holland, 2014), especially in compensated readers (Hoeft et al., 2011; Wang et al., 2016), were compared between groups. These tracts included the right arcuate fasciculus (RAF), inferior longitudinal fasciculus (RILF) and superior longitudinal fasciculus (RSLF). The CC, as the main white matter structure underlying interhemispheric communication, was also examined.

Overall, we hypothesize that if FHD+Typical children develop typical reading skills as a result of a reduced liability, we will not observe different brain mechanisms underlying reading development between FHD− and FHD+ children who subsequently developed

equivalent, typical reading abilities. Alternatively, one can hypothesize that FHD+ children may exhibit neural deficits in the left-hemispheric reading network as a result of their familial risk. However, putative protective pathways might develop prior to reading onset in RH brain regions of FHD+ children through increased interhemispheric functional and structural (CC) connectivity. Such alternative neural mechanisms could facilitate reading development in FHD+ children, resulting in successful reading acquisition in FHD+Typical children.

2 | METHODS

2.1 | General study design

The current study was based on two longitudinal projects in our lab; the "Boston Longitudinal Dyslexia Study" (BOLD) and "Research on the Early Attributes of Dyslexia" (READ) at Boston Children's Hospital (BOLD and READ) and the Massachusetts Institute of Technology (READ). In both projects, children were initially enrolled at the end of the prekindergarten year or the beginning of kindergarten before they started to learn to read (i.e., prereaders), where they completed both behavioral and imaging sessions (more details provided below). All participants were then contacted and invited back to attend a behavioral session every year, in order to track their reading development until the end of second grade (READ) or fourth grade (BOLD). No intervention was administered between annual assessments.

2.2 | Participants

An initial group of 93 participants, including 52 FHD+ children, defined as having at least one first-degree relative with a dyslexia diagnosis, and 41 FHD− controls were retrospectively selected from both longitudinal projects using the following criteria: (a) neural and behavioral data successfully collected at the prereading stage (see below for details); (b) reading skills subsequently assessed at the emergent reading stage. Four standardized word-level reading assessments were applied in the current study, the Word ID (WI) and Word Attack (WA) subtests of the Woodcock Reading Mastery Test-Revised (WRMT-R), Woodcock, 1987), as well as the Sight Word Efficiency (SWE) and Phonemic Decoding Efficiency (PDE) subtests of the Test of Word Reading Efficiency (TOWRE, Torgesen, Rashotte, & Wagner, 1999). Using the criteria of a clinical cutoff of a Standard Score (SS) of 85 in at least one of the four tests at the latest assessment time point, 12 FHD+ (24%) and two FHD− (5%) children can be classified with a reading disability. The prevalence of dyslexia was higher in FHD+ compared to FHD− children ($\chi 2$ [1] = 5.94, p = .015), which was consistent with previous literature (e.g., Boets, Wouters, Van Wieringen, & Ghesquiere, 2007; Torppa et al., 2010; Van Bergen, De Jong, Plakas, Maassen, & van der Leij, 2012). To ensure that participants in the current study were prereaders at the initial stage, eight more children (four FHD−Typical and four FHD+Typical) who identified more than 10 words (25.1 words ± 11.8, range = 11–43) on the WI subtest of the WRMT-R were further excluded. The final

sample included 34 (18 males) FHD−Typical, 35 (18 males) FHD+Typical, and 12 (8 males) FHD+Impaired children. All participants were native English speakers and exhibited nonverbal IQs of SS > 80, as measured by the Kaufman Brief Intelligence Test: Second Edition—Matrices (KBIT-2), Kaufman & Kaufman, 2004). Most children were right handed, with four left-handed children (1 FHD+Typical, 2 FHD−Typical and 1 FHD+Impaired) and one child (FHD−Typical) who did not demonstrate a preference (ambidextrous) also included in the sample. No children reported a history of hearing, vision, psychiatric or neurological disorders. The current study was approved by the institutional review boards at the Massachusetts Institute of Technology and Boston Children's Hospital. Before participation, verbal assent and informed written consent were obtained from each child and guardian, respectively.

2.3 | Longitudinal psychometric measurements

At the prereading stage, the FHD−Typical and FHD+Typical groups did not differ significantly from each other by age (FHD−Typical: 65 ± 4.3 months; FHD+Typical: 66 ± 4.7 months, t_{67} = 1.34; p = .18). However, both groups were on average 4 months younger than the FHD+Impaired group (70 ± 5.6 months; FHD−Typical versus FHD+Impaired: t_{44} = 3.7, p < .001; FHD+Typical versus FHD+Impaired: t_{45} = 2.6, p = .013). All children were assessed on preliteracy skills including (a) phonological processing (the Comprehensive Test of Phonological Processing (CTOPP), Wagner, Torgesen, Rashotte, & Pearson, 1999), which measures the ability to segment, combine and repeat phonological components, (b) rapid automatized naming abilities (RAN, Wolf & Denckla, 2005), which indicates automaticity of phonological access through measuring the amount of time it takes a child to name a series of symbols (e.g., objects and numbers) as fast as possible, and (c) letter knowledge (the Letter Identification subtest of WRMT-R). Their nonverbal IQ (KBIT-2) and word reading abilities (WRMT-R, WI) were also evaluated. Moreover, children from the BOLD project were further examined on their language skills using the Clinical Evaluation of Language Fundamentals: Fourth edition (CELF-4, Semel, Wiig, & Secord, 2003). Home literacy environment (adapted from Denney, English, Gerber, Leafstedt, & Ruz, 2001, Table S1) and socioeconomic status (adapted from the MacArthur Research Network: http://www.macses.ucsf.edu/default.php, Table S2) were characterized based on parent reporting at the first study visit. Children's reading abilities were assessed at the emergent reading stage using the WI and WA subtests of the WRMT-R, as well as the SWE and PDE subtests of the TOWRE. Although the number of acquired time points varied among participants due to scheduling challenges in longitudinal studies (Figure S1), all children included in the current study were successfully assessed at least once after 2 years of formal reading instruction (i.e., the end of first grade). The latest available reading performance for each child (ranging from the end of first to fourth grade) was used for the current analyses. The three groups did not differ in age and school grade associated with the latest available reading performances (grade: $\chi^2[6]$ = 8.0, p = .24; age: $F_{2,78}$ = 0.72, p = .49, see information on grade distribution and age for each group in Table 1).

Raw scores initially acquired from each assessment were converted into standard scores (Mean (M): 100, Standard Deviation (SD): 15; scale scores (M: 10, SD: 3) for the CTOPP results) for result summaries and statistical analyses. To evaluate any potential group differences in behavioral performance, an ANOVA test was carried out for each of the psychometric measures collected at the prereading and emergent reading stages. Similarly, Kruskal–Wallis (nonparametric) tests were performed to evaluate group differences in home literacy environment and socioeconomic status. For any cognitive or environmental measure with a significant group effect ($p < .05$), posthoc pairwise comparisons (t-test

or chi-square) were subsequently conducted. Significant group differences were reported at $p < .05$.

2.4 | Imaging experiment at the prereading stage

2.4.1 | Imaging acquisition

Neuroimaging data collection for the BOLD and READ projects were conducted at Boston Children's Hospital (BCH) and Massachusetts

TABLE 1 Preliteracy characteristics, fMRI experiment performance at the prereading stage, and reading abilities after schooling

	FHD−Typical	FHD+Typical	FHD+Impaired	Group effect
Number (female/male)	34 (16/18)	35 (17/18)	12 (4/8)	
Preliteracy characteristics				
Age (months)	65 ± 4.3[a]	66 ± 4.7[a]	70 ± 5.6[b]	$F_{(2,78)} = 6.69$**
CTOPP: Elision	10 ± 2.1	10 ± 2.4	11 ± 1.8	$F_{(2,75)} = 0.40$
CTOPP: Blending	11 ± 1.9	11 ± 2.2	10 ± 1.7	$F_{(2,75)} = 0.18$
CTOPP: Nonword repetition	9.4 ± 1.6	9.3 ± 2.0	8.9 ± 2.4	$F_{(2,76)} = 0.30$
RAN: Object	104 ± 10[a]	100 ± 13[a]	89 ± 9.9[b]	$F_{(2,71)} = 5.90$**
RAN: Color	101 ± 13	96 ± 17	95 ± 11	$F_{(2,71)} = 0.90$
WRMT-R: Word ID	93 ± 15	96 ± 22	85 ± 7.9	$F_{(2,78)} = 1.47$
KBIT-2: Nonverbal	103 ± 11	99 ± 9.8	104 ± 16	$F_{(2,78)} = 1.36$
CELF-4: Core language	113 ± 14	110 ± 10	108 ± 16	$F_{(2,64)} = 0.75$
CELF-4: Receptive language	111 ± 13	104 ± 15	109 ± 9.1	$F_{(2,65)} = 1.59$
CELF-4: Expressive language	114 ± 14	110 ± 12	107 ± 19	$F_{(2,64)} = 1.12$
CELF-4: Language structure	114 ± 15	110 ± 11	107 ± 17	$F_{(2,63)} = 1.31$
fMRI experiment performance at the prereading stage				
# of correct responses	17 ± 7.2	17 ± 6.3	21 ± 4.3	$F_{(2,65)} = 2.10$
Response times (seconds)	2,336 ± 480	2,170 ± 422	2,143 ± 322	$F_{(2,65)} = 1.34$
Reading abilities at the end of the first grade or later				
# of participants with latest reading performance available in each grade				
First grade	8	5	4	$\chi2_{(6)} = 8.0; p = .24$
Second grade	17	16	5	
Third grade	1	8	1	
Fourth grade	8	6	2	
Age (months)	104 ± 14	108 ± 13	106 ± 15	$F_{(2,78)} = 0.72$
WRMT-R: Word ID	111 ± 9.7[a]	108 ± 10[a]	87 ± 7.0[b]	$F_{(2,76)} = 28.4$***
WRMT-R: Word attack	109 ± 11[a]	109 ± 10[a]	96 ± 11[b]	$F_{(2,76)} = 8.83$***
TOWRE: SWE	109 ± 13[a]	104 ± 9.8[a]	78 ± 8.7[b]	$F_{(2,78)} = 34.6$***
TOWRE: PDE	104 ± 11[a]	104 ± 9.6[a]	86 ± 7.0[b]	$F_{(2,78)} = 17.1$***

Note: Standard scores were reported for all the psychometric assessments. Due to the missing data points in each assessment, degree of freedom and significance level were adjusted accordingly.

For assessments showing significant group effects, posthoc pairwise comparisons were subsequently computed, which revealed a consistent pattern: while no significant differences were observed between the FHD+Typical and FHD−Typical children (both denoted by superscript "a"), both groups were significantly different from FHD+Impaired children (denoted by superscript "b", $p_{corrected} < .05$ after correction for multiple comparisons).

Abbreviations: CELF-4, clinical evaluation of language fundamentals, fourth edition; CTOPP, comprehensive test of phonological processing; FHD+Impaired, children with family history of dyslexia who subsequently developed poor reading abilities; FHD−Typical, children without family history of dyslexia who subsequently developed typical reading abilities; FHD+Typical, children with family history of dyslexia who subsequently developed typical reading abilities; KBIT-2, Kaufman brief intelligence test, second edition—nonverbal matrices; PDE, phonemic decoding efficiency; RAN, rapid automatized naming; SWE, sight word efficiency; TOWRE, test of word reading efficiency; WRMT-R, Woodcock reading mastery tests-revised.

Institute of Technology (MIT), respectively. Images were acquired on a 3 T Siemens Trio Tim MRI scanner with a standard Siemens 32-channel phased array head coil at both sites. For fMRI data collection, a behavioral interleaved gradient imaging design was applied to minimize the influence of scanning background noise during auditory stimulus presentation (Gaab, Gabrieli, & Glover, 2007a, 2007b), using the following parameters: TR = 6,000 ms; TA = 1,995 ms; TE = 30 ms; flip angle = 90°; field-of-view = 256 mm^2; in-plane resolution = 3.125 × 3.125 mm^2, slice thickness = 4 mm, slice gap = 0.8 mm. Structural images were acquired using site-specific specifications as follows: for BCH, slice number = 128, TR = 2000 ms, TE = 3.39 ms, flip angle = 9°, field of view = 256 mm^2, voxel size = 1.3 × 1.0 × 1.3 mm^3; for MIT, slice number = 176, TR = 2,350 ms, TE = 1.64 ms, flip angle = 9°, FOV = 256 mm^2, voxel size 1.0 × 1.0 × 1.0 mm^3. Finally, DTI scans collected at both sites included 10 nondiffusion-weighted volumes (b = 0) and 30 diffusion-weighted volumes acquired with noncolinear gradient directions (b = 1,000 s/mm^2 for BCH and b = 700 s/mm^2 for MIT), all at 128x128 base resolution and isotropic voxel resolution of 2.0 mm^3. Note that DTI data were acquired for only half of the BOLD participants since this sequence was added later during the BOLD recruitment process. Throughout the MRI session, one research assistant accompanied the child participant to ensure minimal head movement and compliance with the task instructions (see detailed protocol in Raschle et al., 2009, 2012).

2.4.2 | Task procedure

A phonological processing task was presented in block design using Presentation software (Version 0.70, www.neurobs.com). During each trial, children saw two common objects presented on the left and right sides of the screen sequentially (2 s for each), while hearing each object's name, spoken in a male or female voice, accompanying its visual appearance. The two pictures stayed on the screen for an additional 2 s, while participants judged whether the first sound of the names of the two objects matched (first sound matching [FSM]) by pressing buttons held in the right (Yes) and left (No) hands. The FSM run was comprised of seven task blocks, each consisting of four trials, alternating with seven fixation blocks of the same length (24 s). A separate experimental run with a control task was constructed with the same stimuli in the same way; however, in this run, participants were asked to decide whether the object names were spoken by the same gender (voice matching [VM]). The experimental and the control tasks were administered in separate runs, as an initial pilot study showed that the youngest participants (62.2–81.6 months) confused the two tasks when they were interleaving within the same run (Raschle, Zuk, Ortiz-Mantilla, et al., 2012). This task has been used by our group numerous times (e.g., Langer, Benjamin, Becker, & Gaab, 2019; Powers, Wang, Beach, Sideridis, & Gaab, 2016; Raschle et al., 2012, 2013; Yu et al., 2018, Zuk et al., 2018), and several other studies have adapted this design for young pediatric populations (e.g., Dębska et al., 2016, 2019). The order of the two runs was counterbalanced across participants (see more details in Raschle et al., 2012, 2013).

2.4.3 | In-scanner performance

Participants' responses were recorded during the neuroimaging sessions. Given the young ages of the participants, self-correction was allowed, and only the last response within each trial was used to compute the number of correct responses and RTs. Group differences in the in-scanner performance were evaluated using ANOVA tests.

2.4.4 | FMRI analyses

fMRI data were successfully collected in 30 FHD−Typical, 30 FHD+Typical and 12 FHD+Impaired children. Consistent with the psychometric session, FHD−Typical and FHD+Typical children did not differ significantly in age during the scanning session (FHD−Typical: 66 ± 4.3 months; FHD+Typical: 68 ± 4.4 months, t_{58} = 1.8; p = .08), but both groups were significantly younger than FHD+Impaired children by 6 months on average (72 ± 5.4 months; FHD−Typical vs. FHD+Impaired: t_{40} = 2.3, p < .05; FHD+Typical vs. FHD+Impaired: t_{40} = 2.3, p < .05). Acquired images were first preprocessed in SPM8 (http://www.fil.ion.ucl.ac.uk/spm/software/spm8), based on Matlab (Mathworks), using an age-appropriate pipeline (Yu, Raney, et al., 2018). Specifically, after removing the initial volumes due to the T1 equilibration effects, functional images were first motion corrected (realigned) and co-registered to the corresponding structural images. Before normalizing fMRI images from the naïve space to the Montreal Neurological Institute (MNI) space, transformational matrices were first estimated for every participant using their corresponding high-resolution structural images in VBM8 (http://www.neuro.uni-jena.de/vbm/). During this step, structural images were segmented into gray matter (GM), white matter (WM), and cerebral spinal fluid (CSF) using an adaptive Maximum A Posterior (MAP) approach (Rajapakse, Giedd, & Rapoport, 1997) and spatially normalized to the MNI space via affine transformation. An age- and gender-matched Tissue Probability Map created using the Template-O-Matic Toolbox (Wilke, Holland, Altaye, & Gaser, 2008) was applied at this stage to accommodate the potential anatomical differences between the brain images of the current pediatric group and MNI templates created based on the adult population (Evans, 1992). A nonlinear normalization step was subsequently performed on the GM and WM, using a diffeomorphic anatomical registration using exponentiated lie algebra (DARTEL) approach (Ashburner, 2007). Another customized template was created based on structural images of 149 children with a similar age (67.9 ± 4.2 months) and gender ratio (Female/Male = 1.04/1) to the current participant group were applied during a DARTEL approach. The linear-transformed GM and WM were mapped to this template through high dimensional warping processes, resulting in optimal registration in local, fine-grained structures among all the participants. The transformational matrices from the native space to the MNI space were generated for each participant after VBM processing and then applied to the corresponding functional images for the normalization purpose. A Gaussian kernel
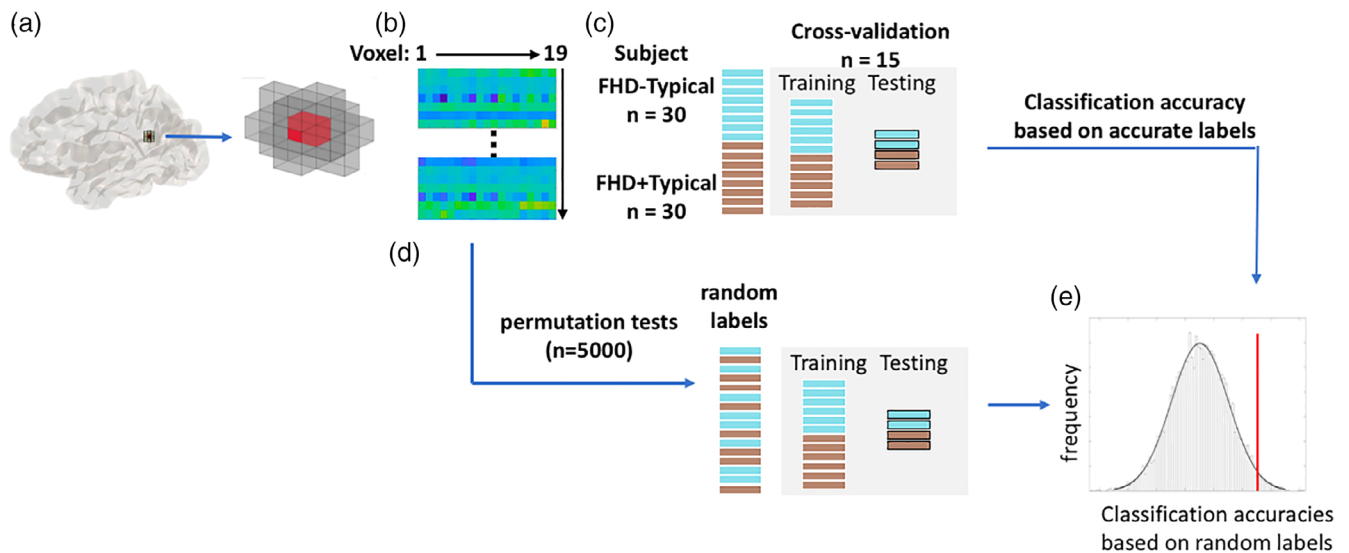
FIGURE 1 Flow chart of a step-by-step procedure of the whole-brain searchlight multivariate pattern analysis. (a) For every voxel (in red), a spherical searchlight was created with a radius of 6 mm (2-voxel radius, resulting in 19 voxels in total). (b) A 19 × 60 matrix was generated using the values derived from the contrast maps for all included voxels and all participants. (c) A linear support vector classifier (SVC, LIBSVM—http://www.csie.ntu.edu.tw/~cjlin/libsvm) was trained and estimated for the classification performance using the generated matrix. To make an unbiased estimation of the classification accuracies, a 15-folder cross-validation approach was adopted. During each iteration, a classifier was trained on 14 folders of subgroups (28 FHD−Typical and 28 FHD+Typical participants) and then used to predict the labels of the remaining folder—that is, 2 FHD−Typical and 2 FHD+Typical. The process was repeated 15 times such that each subject was tested once, and the prediction accuracies of the SVC were estimated across all subjects. (d) Permutation tests (n = 5,000) were subsequently run, in which group labels were randomly assigned to each subject. (e) The significance of the classification accuracy was determined through comparison to the distribution of classification accuracies based on the random labels

with full-width at half maximum (FWHM) of 8 mm was further applied to create smoothed images. Finally, to minimize the effect of head motion on data analyses, Artifact Detection Tools software (http://www.nitrc.org/projects/artifact_detect) was applied to identify scans with excessive motion, using the criterion of displacement of 3 mm (translational) and/or 2° (rotational) from the beginning scan of each run. All the selected images were visually screened, and those with artifacts - such as missing voxels, stripes, ghosting, or intensity differences - were marked as outliers and removed from subsequent analyses. The number of removed scans was not significantly different among the three groups ($F_{2,69}$ = 0.9, p = .4) or two tasks (t_{71} = 1.8, p = .07).

The preprocessed images were then entered into first-level general linear models for estimation of neural responses associated with task conditions (FSM, VM; i.e., regressors of interest). Comprehensive measurements of head motion along three translational and three rotational dimensions combined with the binary regressors representing outlier images were also included as covariates of no interest to minimize the confounding effect of head movement. The potential differences in the motion effect were further evaluated using an overall scalar displacement calculated based on movements of all six directions (Power, Barnes, Snyder, Schlaggar, & Petersen, 2012). This overall measure did not yield any significant differences between different tasks/runs (t_{71} = 0.04, p = .9) or groups ($F_{2,69}$ = 1.1, p = .35). Subject-wise neural responses for phonological processing were estimated by contrasting the beta map of

the FSM condition with that of the VM condition for each participant.

Whole-brain analyses were first carried out with data of FHD+Typical and FHD−Typical children to examine the potential differences in the functional mechanisms underlying phonological processing between prereaders with and without familial risk, despite the comparable and typical reading development. Two approaches were applied here. The first analysis utilized the mass-univariate analysis method to explore whether group differences in activation levels could be observed at the voxel level. To this aim, a two-sample t-test model was built and contrasts between the two groups were tested. In the second analysis, to capture group information embedded in the distributed patterns of brain activity, a searchlight MVPA (Kriegeskorte, Goebel, & Bandettini, 2006) was carried out using the TDT toolbox (Hebart, Görgen, & Haynes, 2015, see Figure 1 for a step-by-step procedure of the whole-brain searchlight MVPA). A linear support vector classifier (SVC, LIBSVM—http://www.csie.ntu.edu.tw/~cjlin/libsvm) was utilized in the current analyses, which aimed to produce a linear boundary separating two categories within a multidimensional space, with the number of dimensions equal to the number of voxels included. In other words, this linear support vector classifier is an analytic technique that surveys the relationships among the voxels (i.e., distributed representation) to identify activation patterns that differentiate experimental conditions (e.g., Friston et al., 1994; Haxby et al., 2001; Norman, Polyn, Detre, & Haxby, 2006). The combination of the MVPA with a searchlight technique further provided

an opportunity for functional localization (Kriegeskorte et al., 2006). Specifically, a spherical searchlight was created for every voxel in the brain with a radius of 6 mm (2-voxel radius, resulting in 19 voxels in total). Then, for each searchlight, the contrast estimates were extracted from all included voxels for each participant, producing a 19*60 matrix. This matrix was fed into a linear support vector classifier, which generated a linear model with an optimal set of weights for all the voxels that could classify the two groups of participants as best as possible. To make an unbiased estimation of the classification accuracies of the linear SVC, a 15-folder cross-validation approach was adopted. All subjects were divided into 15 subgroups, each with two FHD+Typical and FHD−Typical children. During each iteration, a classifier was trained on 14 subgroups (28 FHD−Typical and 28 FHD+Typical participants) and then used to predict the labels of the remaining two pairs. The process was repeated 15 times so that each subject was tested once, and the prediction accuracies of the SVC were estimated across all the subjects. Following Kriegeskorte et al. (2006) and Stelzer, Chen, and Turner (2013), the significance of the classification accuracies was determined by 5,000 permutation tests in which group labels were randomly assigned to each subject for each searchlight. For both analyses, the statistical significances were further FDR-corrected for multiple comparisons, and region with a minimal of five connected voxels (mass-univariate) or searchlights (MVPA) showing $p_{corrected} < .05$ were reported. Moreover, to constrain the analyses to the cerebral cortex, a customized mask was created by overlapping a mean gray matter image (averaged across all the participants and thresholded at .1), with a cerebral mask derived from the Automated Anatomical Labeling atlas (Tzourio-Mazoyer et al., 2002).

The distinct activation patterns between groups could be reflected in the multi-voxel spatial pattern and/or a systemic difference across voxels (Jimura & Poldrack, 2012; Kragel, Carter, & Huettel, 2012). Therefore, follow-up analyses were conducted in regions with significant MVPA results to evaluate whether the potential group differences in activation levels contributed to the distinct activation patterns observed between FHD−Typical and FHD+Typical children (Bauer & Just, 2017; Coutanche, 2013). Since the MVPA considers information across multiple voxels (i.e., activation pattern) as a whole, the subsequent analyses of the group differences in individual voxels were conducted within the context of their contributions to the whole classification model (see a similar analysis in Evans et al., 2014). Specifically, the group differences in the contrast estimates for FSM > VM were computed for every voxel included in each searchlight. Meanwhile, the weight information of every feature (i.e., voxel) in the classification model, representing the classification pattern, was estimated for each significant searchlight using the whole data sets (30 FHD−Typical and 30 FHD+Typical). To account for the dependencies across the neighboring voxels, weight information was further corrected using the covariance matrix among all the voxels included in a searchlight (Haufe et al., 2014). The absolute value of the corrected weight, reflecting the true contribution magnitude of each voxel to the final classification performance, was then correlated with the group difference in activation levels across all the voxels in each searchlight. Statistical significance was held at $p_{corrected} < .05$, corrected for multiple comparisons.

The same classification analyses were further carried out in each identified region as a whole (as compared to the individual searchlights it comprised). Specifically, all the connected searchlights from each significant region were combined into a cluster. The MVPA was performed following the same procedure as that in each searchlight, and the significance of the classification performance was evaluated using the permutation tests ($n = 5,000$). Furthermore, correlation analyses were also performed between the corrected weights of participating voxels and the corresponding voxel-wise group differences, to assess the contribution of differences in the activation levels to distinct patterns between the two groups in each ROI.

Region of interest (ROI) analyses were subsequently performed to evaluate the functional relevance of the identified regions. The whole-brain group comparisons described above enabled the identification of the distinctive neural activation patterns between FHD−Typical and FHD+Typical children. However, as both groups developed equivalent and typical reading skills, it was difficult to tell whether the observed atypical neural activation in FHD+ children reflected a "deficit" as a result of familial risk or a protective mechanism facilitating subsequent reading development. To differentiate between these two possibilities, the classification pattern of each identified region (i.e., the correct weight of each voxel in the classification model) was extracted from the previous regional-based MVPA. This pattern was applied to the data of all FHD+ participants ($n = 42$), including both typical and impaired readers. This operation projected the data point of each subject to the multi-dimensional space, and allowed the calculation of a decision value for each subject, reflecting the distance (a continuous value) to the separating boundary between the two categories. These decision values were then correlated with the reading scores averaged across all four assessments for FHD+ children. The same analyses were repeated for the control subjects (FHD−Typical) for comparison.

Functional connectivity (FC) analyses were next performed to investigate the contribution of the region(s) recruited specifically by the FHD+Typical children to the reading network during phonological processing using the CONN toolbox (Whitfield-Gabrieli & Nieto-Castanon, 2012). The preprocessed functional images were first band-pass filtered (0.008–0.09 Hz), detrended, and denoised to eliminate confounding effects of head movement and global hemodynamic changes using the anatomical aCompCor strategy (Behzadi, Restom, Liau, & Liu, 2007; Chai, Castañón, Öngür, & Whitfield-Gabrieli, 2012). Task-relevant activation was also entered as a covariate of no interest to minimize the artificial interregional correlations caused by the experimental manipulations. Then, the time courses specific to phonological processing were derived through weighting the residual time series by the task regressor specific to the FSM condition. The region(s) that was additionally recruited by the FHD+Typical children, as identified from the whole-brain and ROI-based analyses, was applied as the seed region. Its time course was estimated using principal component analysis. Subject-wise FC maps were generated by correlating the time course of the seed region(s) with the time courses of all remaining voxels, which were subsequently transformed to Fisher's Z-scores. An ANOVA model with FC maps of subjects from the three groups was

constructed at the group level. A left-hemispheric reading network, including the left inferior frontal cortex (pars opercularis and pars triangularis), left superior temporal gyrus, left inferior parietal cortex (inferior parietal lobule and supramarginal gyrus), and left fusiform gyrus was constructed following Preston et al. (2016) and applied as an explicit mask for the group-level analyses. Three pairwise contrasts (FHD+Typical vs. FHD−Typical, FHD+Typical vs. FHD+Impaired, FHD−Typical vs. FHD+Impaired) were built to evaluate any potential group differences in the prereading FC strength between the seed region and left-hemispheric reading network. Significant regions were reported at a cluster-level of $p_{corrected}$ < .05, Monte-Carlo corrected for multiple comparisons (voxel-level p < .005, $k \geq 50$).

2.4.5 | DTI analyses

DTI data was collected in 14 FHD−Typical, 17 FHD+Typical and 8 FHD+Impaired prereaders. The current analyses were focused on FHD+Typical and FHD−Typical, due to failures in reconstructing the target tracts in a sufficient number of FHD+Impaired children (n < 5). No significant differences in age during the scanning session were observed between these two subgroups (FHD−Typical: 66 ± 4.4 months; FHD+Typical: 65 ± 3.7 months, t_{29} = 0.6; p = .5). Consistent with the similar behavioral characteristics between FHD+Typical and FHD−Typical children in the entire sample, these two subgroups did not show any significant differences in preliteracy skills and subsequent reading performance (Table S3).

An established preprocessing protocol appropriate for this age range was applied (Wang et al., 2016). Specifically, a brain mask was first generated for each subject by removing the nonbrain tissue from the corresponding T1 image using the Brain Extraction Tool (Smith, 2002) from Functional MRI of the Brain (FMRIB) software Library (Oxford, UK). Meanwhile, diffusion-weighted images collected in the DICOM format were converted into NRRD format using the DicomToNrrdConverter software (www.slicer.org). The DTIprep software was then applied to detect and correct for artifacts caused by eddy-currents, head motion, bed vibration and pulsation, venetian blind artifacts, as well as slice-wise and gradient-wise intensity inconsistencies (Oguz et al., 2014). Volumes with excessive motion defined as frame-wise head movement larger than 2 mm/0.5° were also identified and excluded from subsequent analyses. The two groups did not differ in head movement for the remaining volumes (three translational movement: left to right: t_{29} = 1.57, p = .13; posterior to anterior: t_{29} = 1.49, p = .15; bottom to top: t_{29} = 1.14, p = .26; three rotational movement: pitch: t_{29} = 1.94, p = .06; roll: t_{29} = 1.38, p = .18; yaw: t_{29} = 0.15, p = .88). The DTI images were further corrected for eddy currents and head motion using the VISTALab diffusion MRI software suite (www.vistalab.com). Diffusion tensors were then fitted using a linear least-squares fit, and FA maps were calculated for all subjects (Basser, Mattiello, & LeBihan, 1994).

Fiber tractography was performed on the white matter tracts of interest using the Automated Fiber-tract Quantification (AFQ)

toolbox (Yeatman, Dougherty, Myall, Wandell, & Feldman, 2012). To do this, deterministic whole-brain streamline tractography was performed using an FA threshold of 0.2 and an angle threshold of 40°. Fibers were then segmented into separate tracts using two predefined anatomical ROIs (back projected from the MNI to the native space via T1 images) per tract as termination points. This was followed by a fiber-tract cleaning procedure to remove branch outliers from the core bundle. Each tract was then sampled to 100 equidistant nodes, and the diffusion property (i.e., the FA value in this case) for each node was estimated using a weighted mean of each fiber's value based on its Mahalanobis distance from the fiber core. The obtained RAF was further aligned using the FA dip along the tract profile, caused by the high curvature and partial voluming with other paths near the temporal–parietal junction (Yeatman et al., 2011). This procedure resulted in 50 nodes of RAF that were commonly shared by most participants. Following this method, the right superior longitudinal fasciculus (RSLF) was successfully identified in 31 children (14 FHD−Typical and 17 FHD+Typical); right inferior longitudinal fasciculus (RILF), in 30 participants (14 FHD−Typical and 16 FHD+Typical); and right arcuate fasciculus (RAF), in 18 subjects (9 FHD−Typical and 9 FHD+Typical). Due to the previously reported difficulties with reproducibility in defining the entire CC (Wakana et al., 2007), FA values were computed only for callosal fibers primarily linking bilateral occipital lobes (CC splenium) and (separately) those connecting frontal lobes (CC genu). Tract reconstruction was successful in the CC genu for 28 children (12 FHD−Typical and 16 FHD+Typical) and in the CC splenium for 26 children (11 FHD−Typical and 15 FHD+Typical).

Two-sample t-tests were first carried out to evaluate FA differences between FHD+Typical and FHD−Typical children at each node in the four identified tracts. For subjects with both fMRI and DTI data available, Pearson-correlation analyses were further performed between functional activation level during phonological processing (i.e., the contrast estimate of FSM > VM) in the region(s) recruited by the FHD+Typical children and FA at each node in all tracts (RSLF: 22 subjects; RILF: 22 subjects; RAF: 12 subjects; CC genu: 20 subjects; and CC splenium: 20 subjects). Significant results were reported at $p_{corrected}$ < .05 for each node, FRD corrected for multiple comparisons.

3 | RESULTS

3.1 | Longitudinal psychometric results

All three groups exhibited equivalent performance on measures of nonverbal IQ (Table 1). FHD+Impaired children scored significantly lower than both the FHD−Typical and FHD+Typical groups on Rapid Automatized Naming for objects (FHD−Typical vs. FHD+Impaired: t_{39} = 3.9, p < .001; FHD+Typical vs. FHD+Impaired: t_{41} = 2.3, p < .05), but not RAN colors. No significant differences were observed for early language competencies, letter knowledge and phonological processing. Finally, no significant group differences were observed

for home literacy environment (HLE) and socio-economic status (SES), except that family members of FHD+Impaired children reportedly wrote letters, cards, diaries, stories, or poems more often than family members of FHD−Typical children (chi-square = 7.2, p < .05; see complete results on HLE and SES in Tables S1 and S2, respectively).

All participants' reading abilities were estimated at the emergent reading stage (between the end of first and fourth grade) after at least 2 years reading instruction. FHD+Typical and FHD−Typical children acquired equivalent scores in all four word-level reading assessments, including the WI and WA subtests of the WRMT-R, as well as the SWE and PDE subtests of the TOWRE. Consistent

with our classification of the groups, FHD+Impaired children exhibited significantly lower performance on all reading measures relative to both FHD+Typical and FHD−Typical children. Moreover, to ensure that the latest time point captured a reliable estimation of reading performance along the developmental trajectory, mean scores of each reading assessment across the performance of all the time points acquired were calculated and subjected to the same analyses as described above. Mean scores were highly correlated with the latest performance for all four assessments (all rs > .95, ps < .001), and demonstrated comparable reading performance between the FHD−Typical and FHD+Typical children, both of which were higher than those of FHD+Impaired children (see Table S4 for more details).

3.2 | FMRI results at the prereading stage

3.2.1 | In-scanner task performance

Behavioral responses from four subjects (three FHD−Typical and one FHD+Typical) could not be recorded due to technical issues. However, their imaging data was still included in analyses, since high performance accuracies were demonstrated during the practice session and consistent button responses were observed by the accompanying research assistant during the formal experiment. Overall, no significant group differences were observed for either accuracy ($F_{2,65}$ = 1.33, p = .27) or reaction time ($F_{2,65}$ = 2.10, p = .13, Table 1).
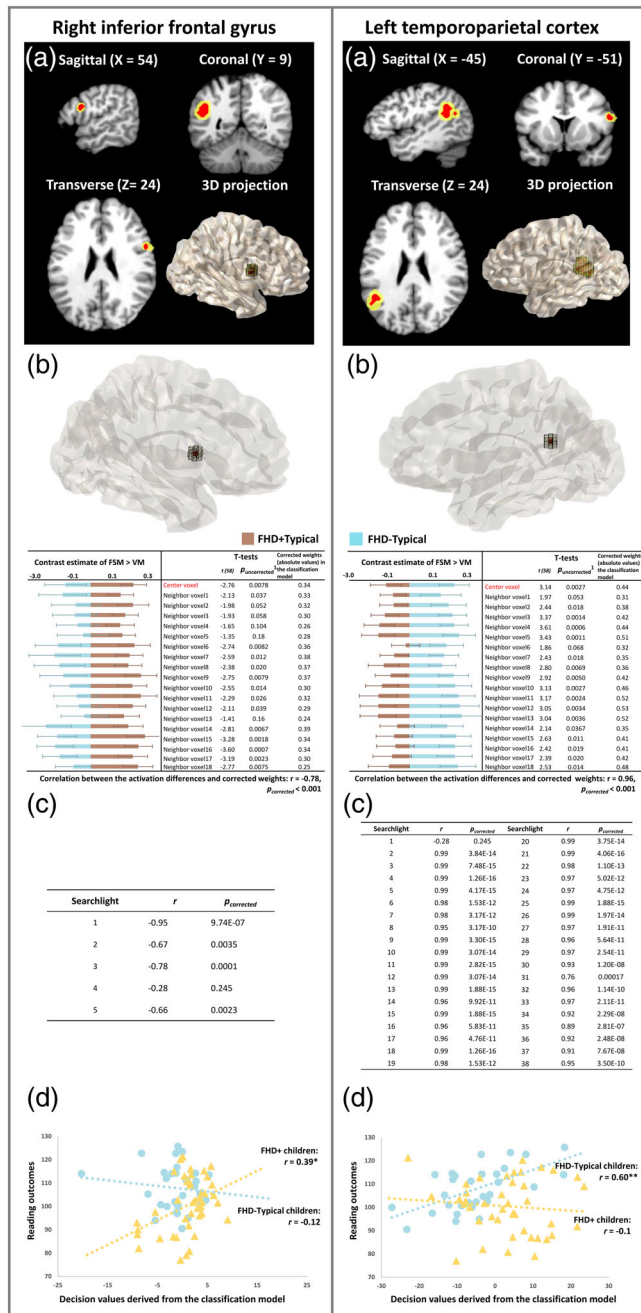

FIGURE 2 The right inferior frontal gyrus (RIFG, left section) and the left temporo-parietal cortex (LTPC, right section) exhibit distinct activation patterns between the FHD−Typical and FHD+Typical children, as revealed by the whole-brain searchlight MVPA. Panel (a) shows RIFG and LTPC in slice-views and 3D projections; the significant regions are highlighted in yellow and the center voxels in red. Panel (b) illustrates that differences between the two groups of children in each voxel included in one example searchlight are significantly correlated with the contribution (corrected weight) of each of those voxels to the classification performance. Each representative searchlight is projected to a 3D image (center voxel in red). The bar figures below the images display the activation levels (contrast estimates of FSM > VM) for FHD+Typical (brown) and FHD−Typical children (blue) in each voxel. The tables show the statistical results of the group comparisons in each voxel and the absolute values of corrected weights in the classification model. Panel (c) summarizes the correlation results for all significant searchlights. Panel (d) shows the correlation results between the decision values derived from the classification models and the subsequent reading outcomes in FHD+ (yellow) and FHD−Typical (blue) children in both RIFG and LTPC regions. Whole-brain results are reported at $p_{corrected}$ < .05, Bonferroni-corrected for multiple comparisons. [1]The results of the two-sample t-tests on the activation levels between the FHD+Typical and FHD−Typical groups in each voxel are not significant after FDR correction ($p_{corrected}$ > .9). $^*p_{corrected}$ < .5; $^{**}p_{corrected}$ < .005

3.3 | FMRI results

3.3.1 | Whole-brain results

Two-sample *t*-tests were first performed at the voxel level throughout the whole brain (i.e., mass-univariate analysis), but no significant differences were observed between the FHD−Typical and FHD+Typical groups (*p* < .05, FDR corrected). The whole-brain searchlight MVPA was subsequently performed, which identified two brain regions exhibiting distinct activation patterns between the FHD−Typical and FHD+Typical children in a combination of neighboring voxels (Figure 2a). The first region was in the right inferior frontal gyrus (RIFG) and comprised five connected searchlights which contained 46 nonoverlapping voxels spanning 1,242 mm^3 of volume (center-of-mass coordinate: [54, 9, 24]). The second region was in the left temporo-parietal cortex (LTPC), including 38 connected searchlights with 200 voxels occupying 5,400 mm^3 of volume (center-of-mass coordinate: [−45, −51, 24]).

Since a searchlight is a joint consideration of 19 neighboring voxels, follow-up analyses were conducted to understand whether the group differences (FHD−Typical > FHD+Typical) in activation levels at each participating voxel contributed to the searchlight to trigger a significant group difference (Coutanche, 2013; Jimura & Poldrack, 2012). Across searchlights, larger group differences in the activation levels contributed more to the classification performance (i.e., higher absolute values of the corrected weights in the classification model, see example searchlights in the Figure 2b). Specifically, for the RIFG, all voxels showed higher activation levels for FHD+Typical than FHD−Typical children. Moreover, activation differences in the participating voxels were significantly and negatively correlated with the corrected weights (absolute values) derived from the classification models in four of five searchlights (r_{mean} = −.76, $p_{corrected\_mean}$ = .0015, Figure 2c). This suggested that distinct activation patterns that reliably distinguished between the two groups in the RIFG region were mainly established on group differences in the FHD+Typical > FHD−Typical direction. By contrast, most of the voxels included in the LTPC searchlights showed higher activation levels for the FHD−Typical compared to the FHD+Typical children (98 ± 8%), and the higher activation levels of FHD−Typical compared to FHD+Typical children were significantly correlated with the higher weights in the classification model in all but one of the 38 searchlights (r_{mean} = .96, $p_{corrected\_mean}$ < .001, Figure 2c). This suggested that the significant differences in activation pattern in the LTPC region were mainly based on group differences in the FHD−Typical > FHD+Typical, a direction opposite to that in the RIFG region.

The same MVPA performed in each region as a whole rendered the same results. Distinct activation patterns were observed between the FHD−Typical and FHD+Typical children in both regions (RIFG: accuracy = 68.3%; $p_{corrected}$ = .016; LTPC: accuracy = 66.7%; $p_{corrected}$ = .02). Moreover, significant correlations were also observed between group differences in the activation levels and corrected weights extracted from the classification model for both regions (RIFG: *r* = −.82; $p_{corrected}$ < .001; LTPC: *r* = .93; $p_{corrected}$ < .001).

3.3.2 | ROI results

Correlation analyses (Figure 2d) further revealed that the decision values of the FHD+ children derived from the activation pattern in RIFG were significantly correlated with their subsequent reading performance (*r* = .39, $p_{uncorrected}$ = .01, $p_{corrected}$ = .04), whereas no such association was observed in LTPC (*r* = −.10, $p_{uncorrected}$ = .99). The opposite pattern was observed for the FHD−Typical children. Specifically, the subsequent reading performance in FHD−Typical children was significantly correlated with the decision values derived from the activation pattern in LTPC (*r* = .60, $p_{uncorrected}$ < .001, $p_{corrected}$ = .0016), but not in RIFG (*r* = −.12, $p_{uncorrected}$ = .52).

3.3.3 | FC results

FC analyses (Figure 3) were conducted to evaluate the functional connection between the putative protective neural region identified in previous analyses and the left-hemispheric reading network. Since the RIFG region showed higher activation for FHD+Typical compared to FHD−Typical children and its activation patterns were positively correlated with subsequent reading performance across all FHD+ children, this region indicated a protective role (see more in discussion) and was chosen as the seed in the current analyses. FC analyses revealed higher FC strength between the RIFG and the left inferior parietal cortex (LIPC), spanning over the left angular gyrus and the left inferior parietal lobule ([−36, −57, 42], *k* = 65 voxels) for the FHD+Typical compared to the FHD−Typical group. Other contrasts did not reveal any significant results.
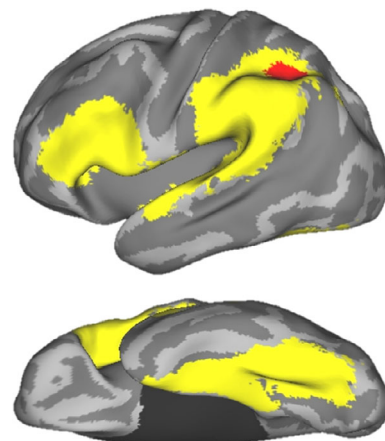

FIGURE 3 Sagittal (top) and transverse (bottom) views of the left hemisphere. Using the RIFG as the seed, functional connectivity (FC) analyses reveal stronger connectivity for FHD+Typical compared to FHD−Typical children in the left inferior parietal cortex (LIPC, highlighted in red) in a pre-defined reading mask (highlighted in yellow), including the inferior frontal cortex, temporo-parietal cortex (both in the sagittal view), and fusiform gyrus (transverse view). Results are reported at cluster-level $p_{corrected}$ < .05, Monte–Carlo corrected for multiple comparisons (voxel-level *p* < .005, *k* ≥ 50)
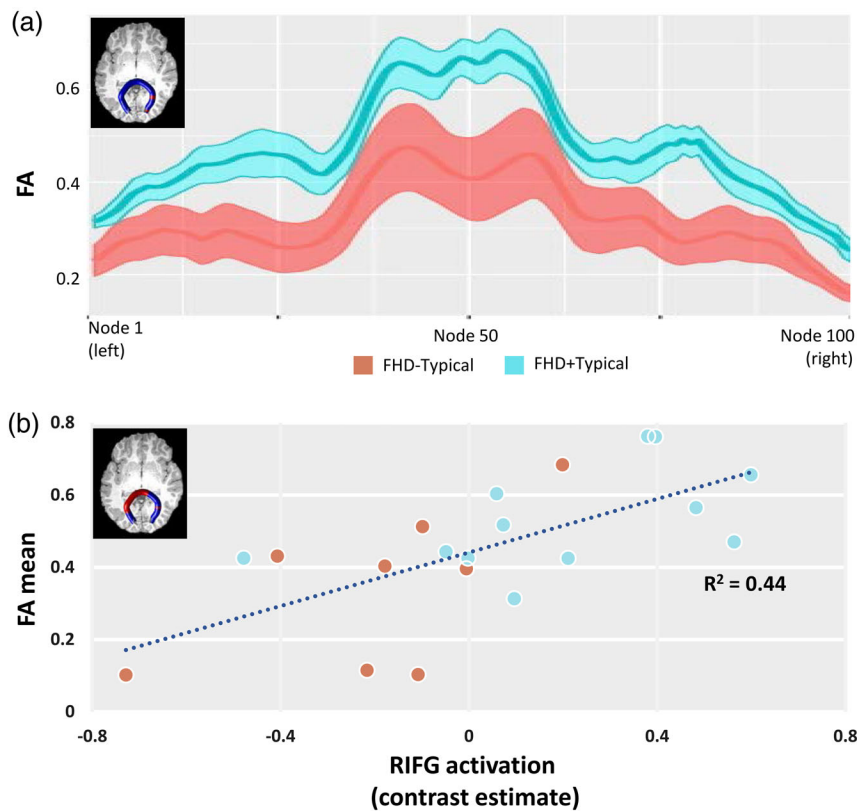
FIGURE 4 Panel (a): Tract profiles (FA values at all 100 nodes) in the corpus callosum (CC) splenium for FHD−Typical (orange) and FHD+Typical (blue) children. Two-sample *t*-tests reveal higher FA values in the right segments of the CC splenium (nodes 77–80 and nodes 96–98, highlighted in red) for the FHD+Typical compared to FHD−Typical children. Panel (b): Correlation plot for mean FA across the significant segments of the corpus callosum splenium (nodes 19–57 and nodes 78–79, highlighted in red) and activation level (contrast estimate of FSM > VM) in right inferior frontal gyrus during the phonological processing task

3.4 | DTI and correlations with fMRI

Significant group differences were observed in the right segments of the CC splenium (nodes 77–80 and nodes 96–98, Figure 4), which demonstrated higher FA for FHD+Typical compared to FHD−Typical children. Group comparisons on the other tract failed to reveal any significant results (Figure S1). Furthermore, correlation analyses between RIFG activation level and FA values at all nodes in all tracts demonstrated positive correlations in the central portion of the CC splenium (nodes 19–57 and nodes 78–79, Figure 4c). No other significant correlations were observed.

4 | DISCUSSION

The current study is the first to demonstrate the presence of putative neural protective mechanisms prior to reading onset in children who subsequently developed typical reading abilities, despite a familial risk for dyslexia. Adopting a retrospective, longitudinal approach, FHD+ children with typical and impaired reading abilities, as well as control subjects (FHD−Typical), were characterized after at least 2 years of reading instruction. Through group comparisons of neural functional characteristics collected before the start of formal reading instruction, distinctive activation patterns were observed between the FHD+Typical and FHD−Typical children, indicating atypical brain mechanisms supporting reading development in FHD+Typical prereaders. These differences were observed despite both groups'

subsequently developing equivalent typical reading abilities. Specifically, the FHD−Typical prereaders showed hypoactivation in the left temporo-parietal cortex (LTPC), whose activation patterns were significantly correlated with the subsequent reading development only in control (FHD−Typical), but not at-risk (FHD+), children. This indicates a neural deficit in LTPC for FHD+Typical children, which is primarily associated with a familial risk rather than a subsequent diagnosis of a reading disability. Meanwhile, higher activations were observed in the right inferior frontal gyrus (RIFG) in FHD+Typical compared to FHD−Typical prereaders, and the activation patterns in RIFG were positively correlated with the subsequent reading development across all FHD+ children, including both typical and impaired readers. Additional analyses on the connectivity characteristics associated with RIFG further revealed increased FC to left inferior parietal cortex (LIPC) and higher FA values of CC in FHD+Typical compared to FHD−Typical children, as well as significant correlation between the FA within CC and activation in RIFG. These multimodal findings together provide strong support for the current hypothesis that neural protective mechanisms may already be established in the right hemisphere in FHD+Typical prereaders, supporting their subsequent typical reading development.

In the current analyses, the searchlight multivariate pattern analysis demonstrated that a combination of voxels can differentiate between FHD−Typical and FHD+Typical children despite no significant group differences observed in individual voxels. As illustrated in the example searchlights in Figure 2b, the neighboring voxels with weak differences in the activation levels (as demonstrated by

$p_{corrected} > .05$) contributed collectively in the searchlight and formed a strong classifier that significantly differentiated across groups. Further looking into the mechanism of how neighboring voxels contributed together in each classification model (Figure 2b,c) has revealed that significant classification results in the RIFG were mainly driven by voxels with higher activation in the FHD+Typical > FHD−Typical direction, while the performance in the LTPC was based on the voxelwise activation in the FHD−Typical > FHD+Typical direction. Therefore, the MVPA exhibited subtle yet consistent and significant activation preferences for the FHD+Typical children in the RIFG and for the FHD−Typical children in the LTPC.

Hypoactivation in the LTPC was observed in FHD+Typical compared to FHD−Typical prereaders despite their subsequent typical reading abilities, underscoring that this is a neural endophenotype associated with familial risk for dyslexia. In the current study, the activation patterns of LTPC at the prereading stage have been shown to significantly correlate with the subsequent reading development in controls (FHD−Typical), supporting the critical role of the left temporo-parietal region in typical phonological processing (e.g., Cattinelli, Borghese, Gallucci, & Paulesu, 2013; Pugh et al., 2001; Schlaggar & McCandliss, 2007). Neural alterations in this region have previously been associated with dyslexia (e.g., Peterson & Pennington, 2015; Richlan et al., 2009; Shaywitz & Shaywitz, 2008) as well as familial risk (e.g., Im et al., 2015; Raschle et al., 2011, 2013; Raschle et al., 2012). Recent effort has been made to disentangle these two effects by comparing FHD+ good and/or poor readers with controls (Hakvoort, van der Leij, Maurits, Maassen, & van Zuijen, 2015; Vanderauwera, Wouters, Vandermosten, & Ghesquière, 2017; Vandermosten et al., 2019). Atypical brain responses for speech and phonological processing were observed in bilateral superior temporal regions in both good and poor readers with a family history when compared to controls, indicating an effect of familial risk (Vandermosten et al., 2019). Our finding further confirmed that this effect exists independently of reading experiences by showing the presence of hypoactivation of the LTPC during phonological processing in FHD+Typical children at the prereading stage. The observed link between LTPC deficits and FHD+ is further supported by recent genome-wide association studies, which have shown significant correlations between variants in dyslexia susceptibility genes and both reading-related functional activation (Cope et al., 2012; Wilcke et al., 2012) and white matter volume (Darki et al., 2012) in LTPC. Due to the probabilistic nature of genetic transmission, it is possible that some FHD+Typical children might develop a typical, left-hemisphere-dominant reading network as a result of reduced/null genetic liability. However, for those FHD+ children who show neural deficits in the LH reading network as observed in the current study (as observed on the group level here), the development of compensatory/protective mechanisms seems to be important for acquiring typical reading skills.

Indeed, greater activation has been observed in the RIFG for FHD+Typical than FHD−Typical prereaders, and its activation patterns were positively correlated with subsequent reading outcomes within all at-risk children, suggesting a potential protective mechanism. Increased activation in the RIFG has been previously associated with reading improvement in individuals with dyslexia and/or reading difficulties, therefore suggesting a compensatory mechanism, perhaps in response to successful intervention approaches (e.g., Eden et al., 2004; Farris et al., 2016; Hoeft et al., 2011; Richards et al., 2007; Temple et al., 2003). The current findings further add to the importance of the RIFG in supporting reading development by demonstrating the establishment of such RH frontal pathways in young FHD+ children prior to reading onset, before the start of any formal reading instruction/practice. This suggests that these RH frontal pathways may serve as a protective mechanism against "adverse" factors such as neural alterations in the LH reading network, and support the typical development of cognitive and preliteracy (e.g., phonological processing) prerequisites for learning to read. This could reduce the likelihood of, or even prevent children from, developing reading impairments including dyslexia. It has been previously shown that structural connectivity precedes the development of the functional reading network (Saygin et al., 2016), suggesting that FHD+Typical children may show an alternative structural connectivity network very early in their language/literacy development (Langer et al., 2017), which then fosters the development of an alternative, protective reading network that enables typical reading development in FHD+Typical children.

As consistent with this conjecture, the protective pathways observed in the right frontal area for the FHD+Typical prereaders were further accompanied by enhanced interhemispheric functional and structural connectivity (CC). Compared to controls (FHD−Typical), FHD+Typical children showed higher FC strength between RIFG and the left inferior parietal cortex, an area that has previously been shown to play an important role in reading development (e.g., Pugh et al., 2000; Schlaggar & McCandliss, 2007). Moreover, they demonstrated higher FA values in CC, the major white matter structure connecting both hemispheres. Most of the CC neurons are excitatory (Fabri, Pierpaoli, Barbaresi, & Polonara, 2014), and their importance for functional interhemispheric connectivity has been demonstrated numerous times (e.g., Cohen et al., 2000; Gooijers & Swinnen, 2014; Mohr, Pulvermüller, Rayman, & Zaidel, 1994). Although the CC has not been investigated in the context of familial risk, it has been associated with the variants of dyslexia susceptibility genes (Darki et al., 2012; Scerri et al., 2012), which might be related to atypical brain development of the CC from an early stage. Therefore, it is possible that higher FA values in the CC observed in FHD+Typical children prior to reading onset might serve as a critical structural foundation that facilitates the recruitment of the right hemisphere during reading development. Similarly, although RH white matter tracts did not yield any significant differences between FHD+Typical and FHD−Typical prereaders in the current study, they did show a significantly higher rate of FA development over the course of learning to read in the RSLF for FHD+ children who subsequently develop into good compared to poor readers based on a partially overlapping sample (Wang et al., 2016). Additionally, the observation of significant correlations between the microstructure of the CC and the neural activation in the RIFG during the phonological processing task further support this hypothesis. Interestingly, our

interpretation is also in line with studies that examined the critical role the CC plays during literacy acquisition in adulthood. These studies showed an increased reliance on bi-hemispheric regions, most likely facilitated through the observed FA increases in the CC, in adults who became literate in their twenties (Carreiras et al., 2009; Dehaene, Cohen, Morais, & Kolinsky, 2015). Nevertheless, since information needs to be transferred across hemispheres, the observed protective/compensatory pathways might support typical reading development at the cost of speed. This speculation is consistent with the observation that FHD+Typical children in general read less fluently than FHD−Typical controls (e.g., Pennington & Lefly, 2001; Van Bergen et al., 2011). Future studies are needed to empirically evaluate the hypothesized association between reading fluency and a bilateral reading network.

Although not directly investigated in the current study, it is important to consider critical factors that might contribute to the emergence of the protective/compensatory mechanisms in FHD+Typical children throughout early development. Investigation of brain characteristics in FHD+ children from an early age suggests an association between familial risk and atypical development of the hemispheric lateralization underlying language and reading development. Compared to a typical left-hemispheric dominance in FHD− controls, FHD+ prereaders and infants exhibit right-lateralized asymmetries in white matter tracts important for reading, as well as bilateral neural activation patterns in response to speech (Guttorm et al., 2001; Leppänen et al., 1999; Wang et al., 2016). The hypothesized genetic influences on atypical brain lateralization in FHD+ children are also in line with the Geschwind-Galaburda hypothesis of early development of atypical lateralization in individuals with dyslexia (Geschwind & Galaburda, 1985), and are further supported by emerging findings suggesting that dyslexia-susceptibility genes are implicated in early brain development, such as cilia function, critical for subsequent hemispheric specialization (Brandler & Paracchini, 2014). Using genome-wide association techniques, dyslexia risk genes have also been directly associated with atypical development of the CC and hemispheric lateralization (Darki et al., 2012; Pinel et al., 2012). Based on these findings, it can be hypothesized that (some) children with a familial risk of dyslexia are genetically predisposed for a bilateral neural mechanism underlying reading development, setting a foundation for the development of RH protective/compensatory functional networks.

Moreover, several environmental factors have also been identified to facilitate the formation of the protective/compensatory functional pathways in the right hemisphere. For example, enriched early home literacy and higher SES have been shown to be associated with enhanced recruitment of right-hemispheric perisylvian and frontal areas for language and reading processing in children (Noble, Wolmetz, Ochs, Farah, & McCandliss, 2006; Powers et al., 2016). Importantly, the association between HLE and neural activation in the right frontal region was specific for FHD+ but not FHD− prereaders (Powers et al., 2016), suggesting a specific gene x environment interaction in the right hemisphere in FHD+ children. In addition to family characteristics, although debated, educational experiences such as musical training and specialized teaching strategies have also been

shown to shape the neural mechanisms underlying reading development toward a bilateral network accompanied with stronger interhemispheric structural microstructure of CC (Habibi, Cahn, Damasio, & Damasio, 2016; Mei et al., 2013; Yoncheva, Blau, Maurer, & McCandliss, 2010; Yoncheva, Wise, & McCandliss, 2015; Zuk et al., 2018). Altogether, one can postulate that positive environmental stimulation, such as enriched home literacy environment, interacts with genetic predisposition, and collectively this may lead to the development of protective/compensatory neural mechanisms in the right hemisphere to mediate the deficient processing in the LH. Thus, this interaction supports typical reading development in FHD+Typical children (Yu, Zuk, & Gaab, 2018).

The presence of distinct neural characteristics in FHD+Typical prereaders compared to controls also provides valuable insight into optimal early diagnosis and intervention approaches. Both neural deficits and putative protective mechanisms were observed in the FHD+Typical children at the prereading stage, encouraging a comprehensive approach that considers both risk and protective aspects when screening for early risk of reading impairment and designing early intervention programs for children at risk for dyslexia (Ozernov-Palchik et al., 2016). Moreover, the establishment of protective pathways prior to reading onset also opens the possibility of developing resilience in at-risk children with preventative intervention approaches administered at early stages of reading development. Children may then experience reduced learning difficulties while learning to read or even exhibit typical reading development, as observed in the FHD+Typical children.

This study provides the first evidence for the development of putative protective neural mechanisms in FHD+ prereaders who subsequently develop typical reading skills, but results are to be interpreted in the context of several considerations. First, the diffusion data was available only in a subsample of the recruited participants. Similar to the entire sample, no significant group differences were observed in preliteracy skills and subsequent reading performance between these subgroups of FHD+Typical and FHD−Typical. However, the generalization of the current results might still be limited due to the small sample size (n = 31), requiring further replication with larger and independent data sets. Second, a small group of FHD+Impaired children (n = 12) were included in the current analyses, limiting the result generalizability. However, it should be noted that the primary analyses have been devoted to characterizing the atypical neural mechanisms underlying reading development in FHD+Typical compared to FHD−Typical children (n = 60), which few studies have investigated (however, see Vandermosten et al., 2019). Future studies with a large sample are needed to determine the exact developmental timelines of compensatory/protective mechanisms that support literacy acquisition in FHD+ children. Finally, the genetic contributions for the development of protective pathways were only tested indirectly in this study, since only children with a reported family history of dyslexia were examined. Future longitudinal studies ranging from infancy to school age are needed and both genetic and environmental measures should be included. These studies will help to identify how early in a child's life these protective neural mechanisms emerge (e.g., are they present at birth or develop over time), and what genetic and

environmental (e.g., home literacy, quality of language input) factors facilitate their emergence over the developmental time course. Answering these research questions could inform the design of preventative and remediation strategies for children at risk for dyslexia.

5 | CONCLUSION

Despite an increased risk of developing dyslexia, about half of children with a familial risk for dyslexia develop typical reading skills. The current study is the first to demonstrate that putative neural protective mechanisms seem to (a) be present before the onset of formal reading instruction and (b) support typical reading abilities in children with a familial risk who subsequently develop typical reading skills. Specifically, compared to controls (FHD−Typical), FHD+Typical prereaders exhibited higher activation in the RIFG during phonological processing and activation patterns within RIFG were positively correlated with subsequent reading outcomes across all FHD+ children. Moreover, the additional recruitment of the RIFG by FHD+Typical was further accompanied by increased interhemispheric functional and structural connectivity. The current findings support a working hypothesis of potential neural protective and compensatory pathways in FHD+Typical children, which may emerge through interactions between genetics, neurobiology, and environmental factors to facilitate typical reading development. Future longitudinal studies are needed to explore the genetic and environmental factors that enable these putative protective and compensatory mechanisms, as well as their developmental trajectories. Such research will guide the design of early assessment and interventional tools for children at risk for dyslexia.

DATA AVAILABILITY STATEMENT
All documentation and codes used in the analysis will be shared upon request. Unfortunately, the consent form used for this study stated that data would not be shared with anyone outside of Boston Children's Hospital (BCH), a former Institutional review Board (IRB) requirement by the institution. We were not able to re-consent the participating families, as the study has ended. However, BCH does allow us to share the data with institutions if a clear data sharing plan is submitted and all data is de-identified. We are willing to work closely on this sharing plan with anyone who would like to re-analyze the data and we will provide templates and procedural outlines.

ORCID
Xi Yu https://orcid.org/0000-0003-0818-1451
Meaghan V. Perdue https://orcid.org/0000-0002-6113-9175
Ola Ozernov-Palchik https://orcid.org/0000-0003-0055-6642
Elizabeth S. Norton https://orcid.org/0000-0002-4023-8051
Yangming Ou https://orcid.org/0000-0002-7726-6208
Nadine Gaab https://orcid.org/0000-0002-7548-413X

REFERENCES
Aboitiz, F., & Montiel, J. (2003). One hundred million years of inter-hemispheric communication: The history of the corpus callosum. *Brazilian Journal of Medical and Biological Research*, 36(4), 409–420.

Ashburner, J. (2007). A fast diffeomorphic image registration algorithm. *Neuroimage*, 38(1), 95–113.

Astrom, R. L., Wadsworth, S. J., & DeFries, J. C. (2007). Etiology of the stability of reading difficulties: The longitudinal twin study of reading disabilities. *Twin Research and Human Genetics*, 10(3), 434–439. https://doi.org/10.1375/twin.10.3.434

Baker, S. F., & Ireland, J. L. (2007). The link between dyslexic traits, executive functioning, impulsivity and social self-esteem among an offender and non-offender sample. *International Journal of Law and Psychiatry*, 30(6), 492–503.

Barquero, L. A., Davis, N., & Cutting, L. E. (2014). Neuroimaging of reading intervention: A systematic review and activation likelihood estimate meta-analysis. *PLoS One*, 9(1), e83668. https://doi.org/10.1371/journal.pone.0083668

Basser, P. J., Mattiello, J., & LeBihan, D. (1994). MR diffusion tensor spectroscopy and imaging. *Biophysical Journal*, 66(1), 259–267.

Bauer, A. J., & Just, M. A. (2017). A brain-based account of "basic-level" concepts. *NeuroImage*, 161, 196–205.

Behzadi, Y., Restom, K., Liau, J., & Liu, T. T. (2007). A component based noise correction method (CompCor) for BOLD and perfusion based fMRI. *NeuroImage*, 37(1), 90–101.

Boets, B., Wouters, J., Van Wieringen, A., & Ghesquiere, P. (2007). Auditory processing, speech perception and phonological ability in pre-school children at high-risk for dyslexia: A longitudinal study of the auditory temporal processing theory. *Neuropsychologia*, 45(8), 1608–1620.

Brandler, W. M., & Paracchini, S. (2014). The genetic relationship between handedness and neurodevelopmental disorders. *Trends in Molecular Medicine*, 20(2), 83–90.

Carreiras, M., Seghier, M. L., Baquero, S., Estévez, A., Lozano, A., Devlin, J. T., & Price, C. J. (2009). An anatomical signature for literacy. *Nature*, 461(7266), 983–986.

Cattinelli, I., Borghese, N. A., Gallucci, M., & Paulesu, E. (2013). Reading the reading brain: A new meta-analysis of functional imaging data on reading. *Journal of Neurolinguistics*, 26(1), 214–238.

Chai, X. J., Castañón, A. N., Öngür, D., & Whitfield-Gabrieli, S. (2012). Anticorrelations in resting state networks without global signal regression. *NeuroImage*, 59(2), 1420–1428.

Cohen, L., Dehaene, S., Naccache, L., Lehéricy, S., Dehaene-Lambertz, G., Hénaff, M.-A., & Michel, F. (2000). The visual word form area: Spatial and temporal characterization of an initial stage of reading in normal subjects and posterior split-brain patients. *Brain*, 123(2), 291–307.

Cope, N., Eicher, J. D., Meng, H., Gibson, C. J., Hager, K., Lacadie, C., … Gruen, J. R. (2012). Variants in the DYX2 locus are associated with altered brain activation in reading-related brain regions in subjects with reading disability. *NeuroImage*, 63(1), 148–156.

Coutanche, M. N. (2013). Distinguishing multi-voxel patterns and mean activation: Why, how, and what does it tell us? *Cognitive, Affective, & Behavioral Neuroscience, 13*(3), 667–673.

Darki, F., Peyrard-Janvid, M., Matsson, H., Kere, J., & Klingberg, T. (2012). Three dyslexia susceptibility genes, DYX1C1, DCDC2, and KIAA0319, affect temporo-parietal white matter structure. *Biological Psychiatry, 72*(8), 671–676.

Dębska, A., Chyl, K., Dzięgiel, G., Kacprzak, A., Łuniewska, M., Plewko, J., ... Jednoróg, K. (2019). Reading and spelling skills are differentially related to phonological processing: Behavioral and fMRI study. *Developmental Cognitive Neuroscience, 39*, 100683.

Dębska, A., Łuniewska, M., Chyl, K., Banaszkiewicz, A., Żelechowska, A., Wypych, M., ... Jednoróg, K. (2016). Neural basis of phonological awareness in beginning readers with familial risk of dyslexia—Results from shallow orthography. *NeuroImage, 132*, 406–416.

Dehaene, S., Cohen, L., Morais, J., & Kolinsky, R. (2015). Illiterate to literate: Behavioural and cerebral changes induced by reading acquisition. *Nature Reviews Neuroscience, 16*(4), 234–244.

Denney, M. K., English, J. P., Gerber, M. M., Leafstedt, J., & Ruz, M. L. (2001). *Family and home literacy practices: Mediating factors for preliterate English learners at risk.* Paper presented at the American Educational Researcher Association Conference, Seattle, WA.

Dougherty, C. (2003). Numeracy, literacy and earnings: Evidence from the National Longitudinal Survey of Youth. *Economics of Education Review, 22*(5), 511–521.

Eden, G. F., Jones, K. M., Cappell, K., Gareau, L., Wood, F. B., Zeffiro, T. A., ... Flowers, D. L. (2004). Neural changes following remediation in adult developmental dyslexia. *Neuron, 44*(3), 411–422.

Evans, A. C. (1992). An MRI-based stereotactic atlas from 250 young normal subjects. *Society for Neuroscience Abstracts, 18*, 408.

Evans, S., Kyong, J. S., Rosen, S., Golestani, N., Warren, J. E., McGettigan, C., ... Scott, S. K. (2014). The pathways for intelligible speech: Multivariate and univariate perspectives. *Cerebral Cortex, 24*(9), 2350–2361.

Fabri, M., Pierpaoli, C., Barbaresi, P., & Polonara, G. (2014). Functional topography of the corpus callosum investigated by DTI and fMRI. *World Journal of Radiology, 6*(12), 895–906.

Farris, E. A., Ring, J., Black, J., Lyon, G. R., & Odegard, T. N. (2016). Predicting growth in word level reading skills in children with developmental dyslexia using an object rhyming functional neuroimaging task. *Developmental Neuropsychology, 41*(3), 145–161.

Friston, K. J., Holmes, A. P., Worsley, K. J., Poline, J. P., Frith, C. D., & Frackowiak, R. S. (1994). Statistical parametric maps in functional imaging: A general linear approach. *Human Brain Mapping, 2*(4), 189–210.

Gaab, N., Gabrieli, J. D., & Glover, G. H. (2007a). Assessing the influence of scanner background noise on auditory processing. I. An fMRI study comparing three experimental designs with varying degrees of scanner noise. *Human Brain Mapping, 28*(8), 703–720.

Gaab, N., Gabrieli, J. D., & Glover, G. H. (2007b). Assessing the influence of scanner background noise on auditory processing. II. An fMRI study comparing auditory processing in the absence and presence of recorded scanner noise using a sparse design. *Human Brain Mapping, 28*(8), 721–732.

Gallagher, A., Frith, U., & Snowling, M. J. (2000). Precursors of literacy delay among children at genetic risk of dyslexia. *The Journal of Child Psychology and Psychiatry and Allied Disciplines, 41*(2), 203–213.

Geschwind, N., & Galaburda, A. M. (1985). Cerebral lateralization: Biological mechanisms, associations, and pathology: I. A hypothesis and a program for research. *Archives of Neurology, 42*(5), 428–459.

Gooijers, J., & Swinnen, S. (2014). Interactions between brain structure and behavior: The corpus callosum and bimanual coordination. *Neuroscience & Biobehavioral Reviews, 43*, 1–19.

Guttorm, T. K., Leppänen, P. H., Richardson, U., & Lyytinen, H. (2001). Event-related potentials and consonant differentiation in newborns with familial risk for dyslexia. *Journal of Learning Disabilities, 34*(6), 534–544.

Habibi, A., Cahn, B. R., Damasio, A., & Damasio, H. (2016). Neural correlates of accelerated auditory processing in children engaged in music training. *Developmental Cognitive Neuroscience, 21*, 1–14.

Haft, S. L., Myers, C. A., & Hoeft, F. (2016). Socio-emotional and cognitive resilience in children with reading disabilities. *Current Opinion in Behavioral Sciences, 10*, 133–141.

Hakvoort, B., van der Leij, A., Maurits, N., Maassen, B., & van Zuijen, T. L. (2015). Basic auditory processing is related to familial risk, not to reading fluency: An ERP study. *Cortex, 63*, 90–103.

Haufe, S., Meinecke, F., Görgen, K., Dähne, S., Haynes, J.-D., Blankertz, B., & Bießmann, F. (2014). On the interpretation of weight vectors of linear models in multivariate neuroimaging. *NeuroImage, 87*, 96–110.

Haxby, J. V., Gobbini, M. I., Furey, M. L., Ishai, A., Schouten, J. L., & Pietrini, P. (2001). Distributed and overlapping representations of faces and objects in ventral temporal cortex. *Science, 293*(5539), 2425–2430.

Hebart, M. N., Görgen, K., & Haynes, J.-D. (2015). The decoding toolbox (TDT): A versatile software package for multivariate analyses of functional imaging data. *Frontiers in Neuroinformatics, 8*, 88.

Hinkley, L. B., Marco, E. J., Brown, E. G., Bukshpun, P., Gold, J., Hill, S., ... Barkovich, A. J. (2016). The contribution of the corpus callosum to language lateralization. *Journal of Neuroscience, 36*(16), 4522–4533.

Hoeft, F., McCandliss, B. D., Black, J. M., Gantman, A., Zakerani, N., Hulme, C., ... Reiss, A. L. (2011). Neural systems predicting long-term outcome in dyslexia. *Proceedings of the National Academy of Sciences, 108*(1), 361–366.

Horowitz-Kraus, T., Wang, Y., Plante, E., & Holland, S. K. (2014). Involvement of the right hemisphere in reading comprehension: A DTI study. *Brain Research, 1582*, 34–44.

Hosseini, S. H., Black, J. M., Soriano, T., Bugescu, N., Martinez, R., Raman, M. M., ... Hoeft, F. (2013). Topological properties of large-scale structural brain networks in children with familial risk for reading difficulties. *NeuroImage, 71*, 260–274.

Im, K., Raschle, N. M., Smith, S. A., Ellen Grant, P., & Gaab, N. (2015). Atypical sulcal pattern in children with developmental dyslexia and at-risk kindergarteners. *Cerebral Cortex, 26*(3), 1138–1148.

International Dyslexia Association. (2007). Dyslexia basics. Retrieved from http://www.interdys.org/ewebeditpro5/upload/Dyslexia_Basics_FS_-_final_81407.pdf.

Jimura, K., & Poldrack, R. A. (2012). Analyses of regional-average activation and multivoxel pattern information tell complementary stories. *Neuropsychologia, 50*(4), 544–552.

Katusic, S. K., Colligan, R. C., Barbaresi, W. J., Schaid, D. J., & Jacobsen, S. J. (2001). *Incidence of reading disability in a population-based birth cohort, 1976-1982.* Paper presented at the Mayo Clinic Proceedings, Rochester, MN.

Kaufman, A. S., & Kaufman, N. L. (2004). *Kaufman Brief Intelligence Test* (2nd ed.). Circle Pines, MN: American Guidance Service.

Koster, C., Been, P. H., Krikhaar, E. M., Zwarts, F., Diepstra, H. D., & Van Leeuwen, T. H. (2005). Differences at 17 months: Productive language patterns in infants at familial risk for dyslexia and typically developing infants. *Journal of Speech, Language, and Hearing Research, 48*(2), 426–438.

Kragel, P. A., Carter, R. M., & Huettel, S. A. (2012). What makes a pattern? Matching decoding methods to data in multivariate pattern analysis. *Frontiers in Neuroscience, 6*, 162.

Kriegeskorte, N., Goebel, R., & Bandettini, P. (2006). Information-based functional brain mapping. *Proceedings of the National Academy of Sciences, 103*(10), 3863–3868.

Langer, N., Benjamin, C., Becker, B. L., & Gaab, N. (2019). Comorbidity of reading disabilities and ADHD: Structural and functional brain characteristics. *Human Brain Mapping, 40*(9), 2677–2698.

Langer, N., Peysakhovich, B., Zuk, J., Drottar, M., Sliva, D. D., Smith, S., ... Gaab, N. (2017). White matter alterations in infants at risk for developmental dyslexia. *Cerebral Cortex, 27*(2), 1027–1036.

Leppänen, P. H., Pihko, E., Eklund, K. M., & Lyytinen, H. (1999). Cortical responses of infants with and without a genetic risk for dyslexia: II. Group effects. *Neuroreport*, 10(5), 969–973.

Lohvansuu, K., Hämäläinen, J. A., Tanskanen, A., Ervast, L., Heikkinen, E., Lyytinen, H., & Leppänen, P. H. (2014). Enhancement of brain event-related potentials to speech sounds is associated with compensated reading skills in dyslexic children with familial risk for dyslexia. *International Journal of Psychophysiology*, 94(3), 298–310.

Lyytinen, H., Ahonen, T., Eklund, K., Guttorm, T., Kulju, P., Laakso, M. L., ... Poikkeus, A. M. (2004). Early development of children at familial risk for dyslexia—Follow-up from birth to school age. *Dyslexia*, 10(3), 146–178.

Lyytinen, H., Ahonen, T., Eklund, K., Guttorm, T. K., Laakso, M.-L., Leinonen, S., ... Puolakanaho, A. (2001). Developmental pathways of children with and without familial risk for dyslexia during the first years of life. *Developmental Neuropsychology*, 20(2), 535–554.

Lyytinen, H., Guttorm, T. K., Huttunen, T., Hämäläinen, J., Leppänen, P. H., & Vesterinen, M. (2005). Psychophysiology of developmental dyslexia: A review of findings including studies of children at risk for dyslexia. *Journal of Neurolinguistics*, 18(2), 167–195.

Maurer, U., Bucher, K., Brem, S., & Brandeis, D. (2003). Altered responses to tone and phoneme mismatch in kindergartners at familial dyslexia risk. *Neuroreport*, 14(17), 2245–2250.

McCandliss, B. D., & Noble, K. G. (2003). The development of reading impairment: A cognitive neuroscience model. *Mental Retardation and Developmental Disabilities Research Reviews*, 9(3), 196–205.

Mei, L., Xue, G., Lu, Z.-L., He, Q., Zhang, M., Xue, F., ... Dong, Q. (2013). Orthographic transparency modulates the functional asymmetry in the fusiform cortex: An artificial language training study. *Brain and Language*, 125(2), 165–172.

Mohr, B., Pulvermüller, F., Rayman, J., & Zaidel, E. (1994). Interhemispheric cooperation during lexical processing is mediated by the corpus callosum: Evidence from the split-brain. *Neuroscience Letters*, 181(1–2), 17–21.

Morgan, P. L., Fuchs, D., Compton, D. L., Cordray, D. S., & Fuchs, L. S. (2008). Does early reading failure decrease children's reading motivation? *Journal of Learning Disabilities*, 41(5), 387–404.

Newbury, D., Paracchini, S., Scerri, T., Winchester, L., Addis, L., Richardson, A. J., ... Monaco, A. (2011). Investigation of dyslexia and SLI risk variants in reading-and language-impaired subjects. *Behavior Genetics*, 41(1), 90–104.

Noble, K. G., Wolmetz, M. E., Ochs, L. G., Farah, M. J., & McCandliss, B. D. (2006). Brain–behavior relationships in reading acquisition are modulated by socioeconomic factors. *Developmental Science*, 9(6), 642–654.

Norman, K. A., Polyn, S. M., Detre, G. J., & Haxby, J. V. (2006). Beyond mind-reading: Multi-voxel pattern analysis of fMRI data. *Trends in Cognitive Sciences*, 10(9), 424–430.

Norton, E. S., Beach, S. D., & Gabrieli, J. D. (2015). Neurobiology of dyslexia. *Current Opinion in Neurobiology*, 30, 73–78.

Oguz, I., Farzinfar, M., Matsui, J., Budin, F., Liu, Z., Gerig, G., ... Styner, M. A. (2014). DTIPrep: Quality control of diffusion-weighted images. *Frontiers in Neuroinformatics*, 8, 4.

Ozernov-Palchik, O., & Gaab, N. (2016). Tackling the 'dyslexia paradox': Reading brain and behavior for early markers of developmental dyslexia. *Wiley Interdisciplinary Reviews: Cognitive Science*, 7(2), 156–176. https://doi.org/10.1002/wcs.1383

Ozernov-Palchik, O., Yu, X., Wang, Y., & Gaab, N. (2016). Lessons to be learned: How a comprehensive neurobiological framework of atypical reading development can inform educational practice. *Current Opinion in Behavioral Sciences*, 10, 45–58.

Pennington, B. F., & Lefly, D. L. (2001). Early reading development in children at family risk for dyslexia. *Child Development*, 72(3), 816–833.

Peterson, R. L., & Pennington, B. F. (2015). Developmental dyslexia. *Annual Review of Clinical Psychology*, 11, 283–307.

Pinel, P., Fauchereau, F., Moreno, A., Barbot, A., Lathrop, M., Zelenika, D., ... Dehaene, S. (2012). Genetic variants of FOXP2 and KIAA0319/TTRAP/THEM2 locus are associated with altered brain activation in distinct language-related regions. *Journal of Neuroscience*, 32(3), 817–825.

Plakas, A., van Zuijen, T., van Leeuwen, T., Thomson, J. M., & van der Leij, A. (2013). Impaired non-speech auditory processing at a pre-reading age is a risk-factor for dyslexia but not a predictor: An ERP study. *Cortex*, 49(4), 1034–1045.

Poelmans, G., Buitelaar, J., Pauls, D., & Franke, B. (2011). A theoretical molecular network for dyslexia: Integrating available genetic findings. *Molecular Psychiatry*, 16(4), 365–382.

Power, J. D., Barnes, K. A., Snyder, A. Z., Schlaggar, B. L., & Petersen, S. E. (2012). Spurious but systematic correlations in functional connectivity MRI networks arise from subject motion. *NeuroImage*, 59(3), 2142–2154.

Powers, S. J., Wang, Y., Beach, S. D., Sideridis, G. D., & Gaab, N. (2016). Examining the relationship between home literacy environment and neural correlates of phonological processing in beginning readers with and without a familial risk for dyslexia: An fMRI study. *Annals of Dyslexia*, 66(3), 337–360.

Preston, J. L., Molfese, P. J., Frost, S. J., Mencl, W. E., Fulbright, R. K., Hoeft, F., ... Pugh, K. R. (2016). Print-speech convergence predicts future reading outcomes in early readers. *Psychological Science*, 27(1), 75–84.

Pugh, K. R., Mencl, W. E., Jenner, A. R., Katz, L., Frost, S. J., Lee, J. R., ... Shaywitz, B. A. (2000). Functional neuroimaging studies of reading and reading disability (developmental dyslexia). *Mental Retardation and Developmental Disabilities Research Reviews*, 6(3), 207–213.

Pugh, K. R., Mencl, W. E., Jenner, A. R., Katz, L., Frost, S. J., Lee, J. R., ... Shaywitz, B. A. (2001). Neurobiological studies of reading and reading disability. *Journal of Communication Disorders*, 34(6), 479–492.

Rajapakse, J. C., Giedd, J. N., & Rapoport, J. L. (1997). Statistical approach to segmentation of single-channel cerebral MR images. *IEEE Transactions on Medical Imaging*, 16(2), 176–186.

Raschle, N., Zuk, J., Ortiz-Mantilla, S., Sliva, D. D., Franceschi, A., Grant, P. E., ... Gaab, N. (2012). Pediatric neuroimaging in early childhood and infancy: Challenges and practical guidelines. *Annals of the New York Academy of Sciences*, 1252(1), 43–50.

Raschle, N. M., Chang, M., & Gaab, N. (2011). Structural brain alterations associated with dyslexia predate reading onset. *NeuroImage*, 57(3), 742–749.

Raschle, N. M., Lee, M., Buechler, R., Christodoulou, J. A., Chang, M., Vakil, M., ... Gaab, N. (2009). Making MR imaging child's play-pediatric neuroimaging protocol, guidelines and procedure. *Journal of Visualized Experiments*, 29, e1309.

Raschle, N. M., Stering, P. L., Meissner, S. N., & Gaab, N. (2013). Altered neuronal response during rapid auditory processing and its relation to phonological processing in prereading children at familial risk for dyslexia. *Cerebral Cortex*, 24(9), 2489–2501.

Raschle, N. M., Zuk, J., & Gaab, N. (2012). Functional characteristics of developmental dyslexia in left-hemispheric posterior brain regions predate reading onset. *Proceedings of the National Academy of Sciences*, 109(6), 2156–2161.

Richards, T., Berninger, V., Winn, W., Stock, P., Wagner, R., Muse, A., & Maravilla, K. (2007). Functional MRI activation in children with and without dyslexia during pseudoword aural repeat and visual decode: Before and after treatment. *Neuropsychology*, 21(6), 732–741.

Richlan, F., Kronbichler, M., & Wimmer, H. (2009). Functional abnormalities in the dyslexic brain: A quantitative meta-analysis of neuroimaging studies. *Human Brain Mapping*, 30(10), 3299–3308.

Richlan, F., Kronbichler, M., & Wimmer, H. (2011). Meta-analyzing brain dysfunctions in dyslexic children and adults. *NeuroImage*, 56(3), 1735–1742. https://doi.org/10.1016/j.neuroimage.2011.02.040

Richlan, F., Kronbichler, M., & Wimmer, H. (2013). Structural abnormalities in the dyslexic brain: A meta-analysis of voxel-based morphometry studies. *Human Brain Mapping*, 34(11), 3055–3065. https://doi.org/10.1002/hbm.22127

Saygin, Z. M., Osher, D. E., Norton, E. S., Youssoufian, D. A., Beach, S. D., Feather, J., ... Kanwisher, N. (2016). Connectivity precedes function in the development of the visual word form area. *Nature Neuroscience, 19*(9), 1250–1255.

Scarborough, H. S. (1990). Very early language deficits in dyslexic children. *Child Development, 61*(6), 1728–1743.

Scerri, T. S., Darki, F., Newbury, D. F., Whitehouse, A. J., Peyrard-Janvid, M., Matsson, H., ... Stein, J. (2012). The dyslexia candidate locus on 2p12 is associated with general cognitive ability and white matter structure. *PLoS One, 7*(11), e50321.

Scerri, T. S., Morris, A. P., Buckingham, L.-L., Newbury, D. F., Miller, L. L., Monaco, A. P., ... Paracchini, S. (2011). DCDC2, KIAA0319 and CMIP are associated with reading-related traits. *Biological Psychiatry, 70*(3), 237–245.

Schlaggar, B. L., & McCandliss, B. D. (2007). Development of neural systems for reading. *Annual Review of Neuroscience, 30*, 475–503. https://doi.org/10.1146/annurev.neuro.28.061604.135645

Semel, E., Wiig, E. H., & Secord, W. A. (2003). *Clinical evaluation of language fundamentals, (CELF-4)*. San Antonio, TX: The Psychological Corporation.

Shaywitz, S. E., & Shaywitz, B. A. (2008). Paying attention to reading: The neurobiology of reading and dyslexia. *Development and Psychopathology, 20*(4), 1329–1349.

Shaywitz, S. E., Shaywitz, B. A., Fulbright, R. K., Skudlarski, P., Mencl, W. E., Constable, R. T., ... Fletcher, J. M. (2003). Neural systems for compensation and persistence: Young adult outcome of childhood reading disability. *Biological Psychiatry, 54*(1), 25–33.

Smith, S. M. (2002). Fast robust automated brain extraction. *Human Brain Mapping, 17*(3), 143–155.

Snowling, M. J., Gallagher, A., & Frith, U. (2003). Family risk of dyslexia is continuous: Individual differences in the precursors of reading skill. *Child Development, 74*(2), 358–373.

Snowling, M. J., & Melby-Lervåg, M. (2016). Oral language deficits in familial dyslexia: A meta-analysis and review. *Psychological Bulletin, 142*(5), 498. https://doi.org/10.1037/bul0000037

Stelzer, J., Chen, Y., & Turner, R. (2013). Statistical inference and multiple testing correction in classification-based multi-voxel pattern analysis (MVPA): Random permutations and cluster size control. *NeuroImage, 65*, 69–82.

Taipale, M., Kaminen, N., Nopola-Hemmi, J., Haltia, T., Myllyluoma, B., Lyytinen, H., ... Hannula-Jouppi, K. (2003). A candidate gene for developmental dyslexia encodes a nuclear tetratricopeptide repeat domain protein dynamically regulated in brain. *Proceedings of the National Academy of Sciences, 100*(20), 11553–11558.

Temple, E., Deutsch, G. K., Poldrack, R. A., Miller, S. L., Tallal, P., Merzenich, M. M., & Gabrieli, J. D. (2003). Neural deficits in children with dyslexia ameliorated by behavioral remediation: Evidence from functional MRI. *Proceedings of the National Academy of Sciences, 100*(5), 2860–2865.

Torgesen, J. K., Rashotte, C. A., & Wagner, R. K. (1999). *TOWRE: Test of word reading efficiency*. Austin, TX: Pro-Ed.

Torppa, M., Lyytinen, P., Erskine, J., Eklund, K., & Lyytinen, H. (2010). Language development, literacy skills, and predictive connections to reading in Finnish children with and without familial risk for dyslexia. *Journal of Learning Disabilities, 43*(4), 308–321. https://doi.org/10.1177/0022219410369096

Tzourio-Mazoyer, N., Landeau, B., Papathanassiou, D., Crivello, F., Etard, O., Delcroix, N., ... Joliot, M. (2002). Automated anatomical labeling of activations in SPM using a macroscopic anatomical parcellation of the MNI MRI single-subject brain. *NeuroImage, 15*(1), 273–289.

Van Bergen, E., De Jong, P. F., Plakas, A., Maassen, B., & van der Leij, A. (2012). Child and parental literacy levels within families with a history of dyslexia. *Journal of Child Psychology and Psychiatry, 53*(1), 28–36.

Van Bergen, E., De Jong, P. F., Regtvoort, A., Oort, F., Van Otterloo, S., & van der Leij, A. (2011). Dutch children at family risk of dyslexia: Precursors, reading development, and parental effects. *Dyslexia, 17*(1), 2–18.

van der Leij, A., Van Bergen, E., van Zuijen, T., De Jong, P., Maurits, N., & Maassen, B. (2013). Precursors of developmental dyslexia: An overview of the longitudinal Dutch dyslexia programme study. *Dyslexia, 19*(4), 191–213.

van Herten, M., Pasman, J., van Leeuwen, T. H., Been, P. H., van der Leij, A., Zwarts, F., & Maassen, B. (2008). Differences in AERP responses and atypical hemispheric specialization in 17-month-old children at risk of dyslexia. *Brain Research, 1201*, 100–105.

van Leeuwen, T., Been, P., Kuijpers, C., Zwarts, F., Maassen, B., & van der Leij, A. (2006). Mismatch response is absent in 2-month-old infants at risk for dyslexia. *Neuroreport, 17*(4), 351–355.

van Leeuwen, T., Been, P., van Herten, M., Zwarts, F., Maassen, B., & van der Leij, A. (2007). Cortical categorization failure in 2-month-old infants at risk for dyslexia. *Neuroreport, 18*(9), 857–861.

Vanderauwera, J., Wouters, J., Vandermosten, M., & Ghesquière, P. (2017). Early dynamics of white matter deficits in children developing dyslexia. *Developmental Cognitive Neuroscience, 27*, 69–77.

Vandermosten, M., Correia, J., Vanderauwera, J., Wouters, J., Ghesquière, P., & Bonte, M. (2019). Brain activity patterns of phonemic representations are atypical in beginning readers with family risk for dyslexia. *Developmental Science, 23*, e12857.

Vandermosten, M., Vanderauwera, J., Theys, C., De Vos, A., Vanvooren, S., Sunaert, S., ... Ghesquière, P. (2015). A DTI tractography study in pre-readers at risk for dyslexia. *Developmental Cognitive Neuroscience, 14*, 8–15.

Wagner, R. K., Torgesen, J. K., Rashotte, C. A., & Pearson, N. A. (1999) *Comprehensive test of phonological processing: CTOPP*. Austin, TX: Pro-ed.

Wakana, S., Caprihan, A., Panzenboeck, M. M., Fallon, J. H., Perry, M., Gollub, R. L., ... Dubey, P. (2007). Reproducibility of quantitative tractography methods applied to cerebral white matter. *NeuroImage, 36*(3), 630–644.

Wang, Y., Mauer, M. V., Raney, T., Peysakhovich, B., Becker, B. L., Sliva, D. D., & Gaab, N. (2016). Development of tract-specific white matter pathways during early reading development in at-risk children and typical controls. *Cerebral Cortex, 27*(4), 2469–2485.

Whitfield-Gabrieli, S., & Nieto-Castanon, A. (2012). Conn: A functional connectivity toolbox for correlated and anticorrelated brain networks. *Brain Connectivity, 2*(3), 125–141.

Wilcke, A., Ligges, C., Burkhardt, J., Alexander, M., Wolf, C., Quente, E., ... Müller-Myhsok, B. (2012). Imaging genetics of FOXP2 in dyslexia. *European Journal of Human Genetics, 20*(2), 224–229.

Wilke, M., Holland, S. K., Altaye, M., & Gaser, C. (2008). Template-O-Matic: A toolbox for creating customized pediatric templates. *NeuroImage, 41*(3), 903–913.

Wolf, M., & Denckla, M. B. (2005). *RAN/RAS: Rapid automatized naming and rapid alternating stimulus tests*. Austin, TX: Pro-Ed.

Woodcock, R. W. (1987). *Woodcock reading mastery tests, revised*. Circle Pines, MN: American Guidance Service.

Yeatman, J. D., Dougherty, R. F., Myall, N. J., Wandell, B. A., & Feldman, H. M. (2012). Tract profiles of white matter properties: Automating fiber-tract quantification. *PLoS One, 7*(11), e49790.

Yeatman, J. D., Dougherty, R. F., Rykhlevskaia, E., Sherbondy, A. J., Deutsch, G. K., Wandell, B. A., & Ben-Shachar, M. (2011). Anatomical properties of the arcuate fasciculus predict phonological and reading skills in children. *Journal of Cognitive Neuroscience, 23*(11), 3304–3317.

Yoncheva, Y. N., Blau, V. C., Maurer, U., & McCandliss, B. D. (2010). Attentional focus during learning impacts N170 ERP responses to an artificial script. *Developmental Neuropsychology, 35*(4), 423–445.

Yoncheva, Y. N., Wise, J., & McCandliss, B. (2015). Hemispheric specialization for visual words is shaped by attention to sublexical units during initial learning. *Brain and Language, 145*, 23–33. https://doi.org/10.1016/j.bandl.2015.04.001

Yu, X., Raney, T., Perdue, M. V., Zuk, J., Ozernov-Palchik, O., Becker, B. L., … Gaab, N. (2018). Emergence of the neural network underlying phonological processing from the prereading to the emergent reading stage: A longitudinal study. *Human Brain Mapping*, *39*(5), 2047–2063.

Yu, X., Zuk, J., & Gaab, N. (2018). What factors facilitate resilience in developmental dyslexia? Examining protective and compensatory mechanisms across the neurodevelopmental trajectory. *Child Development Perspectives*, *12*(4), 240–246.

Zuk, J., Perdue, M. V., Becker, B., Yu, X., Chang, M., Raschle, N. M., & Gaab, N. (2018). Neural correlates of phonological processing: Disrupted in children with dyslexia and enhanced in musically trained children. *Developmental Cognitive Neuroscience*, *34*, 82–91.

SUPPORTING INFORMATION

Additional supporting information may be found online in the Supporting Information section at the end of this article.